BIOCHEMISTRY
including biophysical chemistry & molecular biology

Current Topic

pubs.acs.org/biochemistry

Alternative Conformations of Cytochrome *c*: Structure, Function, and Detection

Luciana Hannibal,[†,‡,§] Florencia Tomasina,[†,‡] Daiana A. Capdevila,[∥] Verónica Demicheli,[†,‡] Verónica Tórtora,[†,‡] Damián Alvarez-Paggi,[∥] Ronald Jemmerson,[⊥] Daniel H. Murgida,[∥] and Rafael Radi*[,†,‡]

[†]Departamento de Bioquímica, Facultad de Medicina, Universidad de la República, Avda. General Flores 2125, 11800 Montevideo, Uruguay

[‡]Centro de Investigaciones Biomédicas (CEINBIO), Facultad de Medicina, Universidad de la República, Avda. General Flores 2125, 11800 Montevideo, Uruguay

[§]Center for Pediatrics and Adolescent Medicine, Medical Center, University of Freiburg, Mathildenstrasse 1, Freiburg D-79106, Germany

[∥]Departamento de Química Inorgánica, Analítica y Química Física/INQUIMAE, Facultad de Ciencias Exactas y Naturales, Universidad de Buenos Aires, Pabellón 2, Ciudad Universitaria, C1428EHA Buenos Aires, Argentina

[⊥]Department of Microbiology and Immunology, University of Minnesota, MMC 196, 420 Delaware Street, Southeast, Minneapolis, Minnesota 55455, United States

ABSTRACT: Cytochrome *c* (cyt *c*) is a cationic hemoprotein of ~100 amino acid residues that exhibits exceptional functional versatility. While its primary function is electron transfer in the respiratory chain, cyt *c* is also recognized as a key component of the intrinsic apoptotic pathway, the mitochondrial oxidative protein folding machinery, and presumably as a redox sensor in the cytosol, along with other reported functions. Transition to alternative conformations and gain-of-peroxidase activity are thought to further enable the multiple functions of cyt *c* and its translocation across cellular compartments. *In vitro*, direct interactions of cyt *c* with cardiolipin, post-translational modifications such as tyrosine nitration, phosphorylation, methionine sulfoxidation, mutations, and even fine changes in electrical fields lead to a variety of conformational states that may be of biological relevance. The identification of these alternative conformations and the elucidation of their functions *in vivo* continue to be a major challenge. Here, we unify the knowledge of the structural flexibility of cyt *c* that supports functional moonlighting and review biochemical and immunochemical evidence confirming that cyt *c* undergoes conformational changes during normal and altered cellular homeostasis.

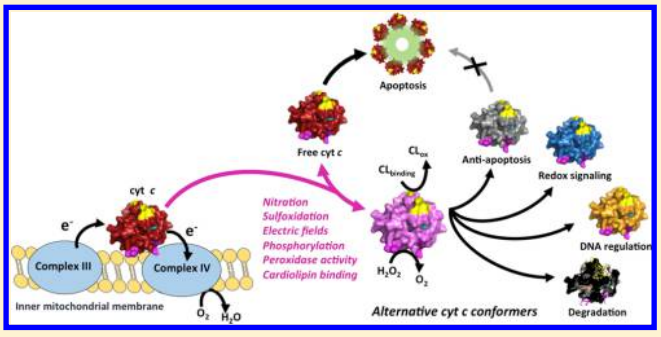

Cytochrome *c* (cyt *c*) is a globular hemoprotein composed of 94−114 amino acid residues depending on the species.[1−3] During the early stages of evolution, anthropoid cyt *c* underwent accelerated changes in its primary sequence, and this was mirrored by mutations in the cyt *c* binding site of cyt *c* oxidase.[4] These early changes in sequence optimized the rates of electron transfer to meet increased demands of cellular respiration.[4] Phylogenetic analysis showed that the rate of cyt *c* evolution has slowed steeply thereafter, and that more recent versions of the protein as seen in new world monkeys and humans are markedly resistant to mutational change.[1,4] Further, a search for natural variants of human cyt *c* revealed that the gene is essentially monomorphic.[5] In particular, a high degree of sequence conservation has been noted in the N- and C-termini of cyt *c*, with presumptive roles in the early events of protein folding and maturation.[6−9] Amino acid residues forming helical structures at the N-terminus of cyt *c* are essential for recognition by holo-cyt *c* synthetase during protein maturation.[10]

Only 15 amino acid residues, namely, Cys14, Cys17, His18, Gly29, Pro30, Gly41, Asn52, Trp59, Tyr67, Leu68, Pro71, Pro76, Thr78, Met80, and Phe82, have been conserved in evolution to support essential structural and functional roles.[3,11] Residues Cys14 and Cys17 are necessary for thioether bonding with the heme moiety (Figure 1a).[12] Residues His18 and Met80 coordinate the heme axially, providing the appropriate redox potential for electron transfer to cyt *c* oxidase in the respiratory chain ($E°$ = 260 mV).[13] Tyr67 donates a hydrogen bond to the Fe−S bond, to further tune electron transfer reactions. As will be shown, early observations by Margoliash and colleagues suggested that conserved residue Tyr67 survived

Received: November 6, 2015
Published: December 31, 2015

DOI: 10.1021/acs.biochem.5b01385
Biochemistry 2016, 55, 407−428

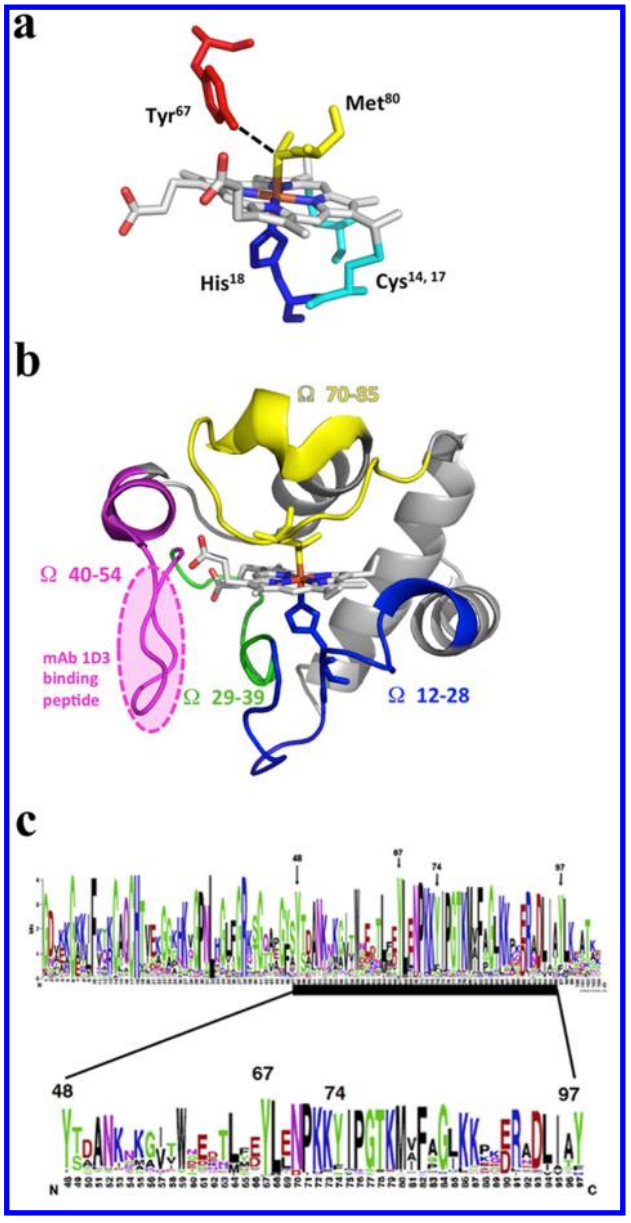

Figure 1. Structure of cyt *c*. (a) Active site of human cyt *c* variant G41S (PDB entry 3NWV) showing axial residues Met80 and His18, thioether-linked Cys14 and -17, and residue Tyr67 forming a H-bond with Fe−S-linked Met80. (b) Three-dimensional structure of human cyt *c* variant G41S (PDB entry 3NWV). The most flexible loop comprising amino acid residues 70−85 is colored yellow. The recognition site of mAb 1D3 comprising residues 40−54 is colored magenta. (c) Amino acid composition of eukaryotic cyt *c* proteins. The numbers indicate the positions of conserved tyrosine residues (reprinted from ref 11. Copyright 2011 Elsevier). The height of each residue correlates with a greater level of conservation across species.

mutational replacement to preserve molecular flexibility.[14] With the exception of Tyr67, all the residues anchoring the heme moiety belong to highly mobile strands of amino acids termed omega (Ω) loops (Figure 1b). Residue Asn52 constitutes one of three putative sites (sites A, C, and L) for the association of cardiolipin (CL) to cyt *c*.[15] At physiological pH, cyt *c* possesses an overall charge of +8 (pI = 10.2−10.5).[16] This facilitates its interaction with negatively charged molecules, such as the phospholipid CL. CL mediates the anchoring of cyt *c* to the inner mitochondrial membrane for electron transfer during respiration and also partakes in redox signaling in a step preceding apoptosis.[17] Specifically, oxidation of CL decreases its affinity for cyt *c*; this enriches the pool of free cyt *c* in the intermembrane space, priming its release into the cytosol prior to caspase activation.[17]

Cyt *c* participates in the next to final step of cellular respiration by transferring electrons to cyt *c* oxidase, which reduces dioxygen to form water and, ultimately, ATP.[13] Native cyt *c* also participates in the mitochondrial oxidative pathway of protein folding by receiving electrons from the Mia40-Erv1 pair.[18] This pathway targets newly made proteins into the intermembrane space for folding coupled to oxidation via formation of disulfide bonds.[18]

Alkaline pH and certain biochemical and biophysical cellular factors induce the so-called "alkaline transition"[19−21] to alternative, non-native conformations of cyt *c* whose biological functions are a matter of intense investigation. In the alkaline transition, rupture of Fe−Met ligation leads to replacement of the Met ligand with an ε-amino group from a Lys residue or additional surrogate ligands, a reduction in midpoint potential, gain-of-peroxidase activity, and ultimately the release of cyt *c* from the mitochondrion to the cytosol. This process influences cellular homeostasis and stress responses via the generation of cyt *c* species that can readily interact with CL and cellular peroxides[22,23] and facilitation of translocation of cyt *c* into the cytosol and nucleus,[24] which can participate in cell signaling events. Substitution of Met80 with Lys is thought to increase the accessibility of hydrogen peroxide and other peroxides to the heme center to support peroxidase activity. Factors that trigger partial unfolding of cyt *c* such as phospholipid binding, pH, and ionic strength culminate in displacement of the Met axial ligand, turning the protein into a peroxidase.[25−27] Mutations of neighboring nonaxial residues have also been shown to increase the peroxidase activity of cyt *c* by destabilizing the Fe−Met bond, hence facilitating the alkaline transition.[28] Human cyt *c* possesses five Tyr residues, Tyr46, Tyr48, Tyr67, Tyr74, and Tyr97, four of which are highly conserved across species (Figure 1c).[11] Tyrosine residues serve as substrates for post-translational modifications and tune the redox properties and peroxidase activity of cyt *c*.[29] Nitration of Tyr residues in cyt *c* has been shown to induce an "early" alkaline transition with a gain of peroxidase activity.[30] Mouse and human G41S variants of cyt *c* display an increased peroxidase activity without prior loss of the Fe−Met80 bond.[31] Replacement of Gly with Ser in position 41 alters the H-bond network of the region comprising amino acid residues 40−57, impairing its interactions with the heme center.[31] The respective contributions of the G41S mutation and the presence of bound cardiolipin were similar, and not additive, suggesting a shared mechanism for the enhancement of peroxidase activity. A second naturally occurring mutation of the human cyt *c* gene was identified (Y48H), resulting in biological effects similar to those observed in patients carrying the G41S mutation.[32] The yeast iso-cyt *c* variant Y48H was reported to exhibit a decreased midpoint potential (approximately −80 mV compared to wild-type iso-cyt *c*).[33] A complete biophysical characterization of human and yeast counterparts of variant Y48H is required to fully comprehend their behavior toward CL binding, electron transfer, and other redox processes.

The peroxidase activity of cyt *c* has been shown to be critical for the release of this and other proteins from mitochondria

DOI: 10.1021/acs.biochem.5b01385
Biochemistry 2016, 55, 407−428

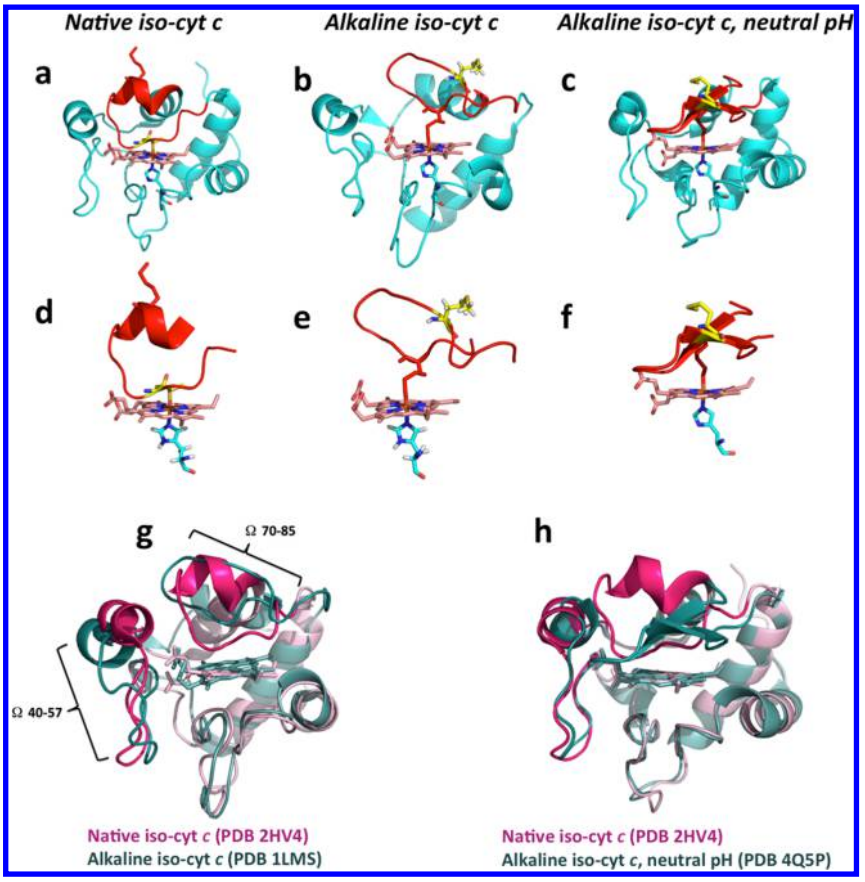

Figure 2. Comparison of native and alkaline cyt *c*. (a) At neutral pH, the heme center of yeast iso-cyt *c* is coordinated axially by His18 and Met80. (b) An increase in pH leads to formation of an alkaline conformer Lys73−Fe−His18 that exhibits significant rearrangement of loop 70−85. (c) Alkaline cyt *c* also exists at neutral pH. The structure is compact, although the heme ligating loop 70−85 rearranges to form a β-hairpin structure. Panels d−f highlight the heme axial ligation, side chains, and loop 79−85 in each variant of yeast iso-cyt *c* presented above. Lys73 is shown as red sticks in native cyt *c* (d), whereas displaced Met80 is shown as yellow sticks in the alkaline conformers (e and f). Panels g and h show a superposition of native and alkaline conformers of yeast iso-cyt *c*. In both cases, substantial conformational change is observed for loop 70−85. The alkaline conformer obtained at high pH (g) presents a looser structure, a slightly different disposition of heme side chains, and a more marked distortion of loop 40−57 compared to those of the alkaline conformer crystallized at neutral pH (h).

early in apoptosis.[34] Studies performed with a recombinant variant Met80Ala showed that this mutant cyt *c* had an increased peroxidase activity and translocated more readily into the cytoplasm and nucleolus even under nonapoptotic conditions.[24] Disruption of the coordination environment by heme nitrosylation occurs under apoptotic conditions.[35] Nitrosylated cyt *c* was recovered from cytosol extracts, suggesting that this alternative conformation translocated across the mitochondrial membrane.[35] X-ray crystallographic analysis of native yeast iso-1 cyt *c* in comparison to its alkaline transition state with acquisition of peroxidase activity shows a dramatic change in conformation (Figure 2). Biochemical data indicate that similar structural differences exist between the native and alkaline transition states of mammalian cyts *c*. A monoclonal antibody (mAb), mAb 1D3, specific for a non-native form of mammalian cyt *c* that recognizes the alkaline transition state as well as phospholipid-bound cyt *c* and does not recognize native cyt *c* has been shown to label mitochondria in cells at an early stage of apoptosis prior to the acquisition of characteristics that define the apoptotic state.[36] This indicates that a conformational change in cyt *c*, likely indicative of the peroxidase-active conformation obtained through its association with cardiolipin, does occur in cells. In mammals, cyt *c* released from the mitochondrion participates in the oligomerization of Apaf-1, which in turn leads to activation of pro-caspase 9, a key enzyme activating apoptosis.[37] Cyt *c* in complex with Apaf-1 appears to be native, suggesting that the conformational change occurring in mitochondria is reversible. Cryo-electron microscopy studies at near atomic resolution revealed that cyt *c* releases the autoinhibition of Apaf-1 via specific interaction with its WD40 repeats (also known as β-transducin repeats).[38] This study also showed that amino acid residues Gly56, Lys72, Pro76, and Ile81 of cyt *c* are critical for its association with Apaf-1 via H-bonding interactions and that assembly of the apoptosome requires the simultaneous presence of cyt *c*, Apaf-1, and ATP.[38]

Other binding partners for cyt *c* and putative functions have been identified. These include binding of cyt *c* to inositol 1,4,5-triphosphate receptors in the endoplasmic reticulum to effect calcium release,[39] interaction with cytosolic heat shock protein 27 to block apoptosis induction,[40] and binding to extracellular leucine-rich α-2-glycoprotein-1 to extend cell survival under stress conditions.[41] It is not known if a gain of peroxidase function through conformational alteration plays a role in these functions. Further, it remains to be elucidated whether the alternative conformations of cyt *c* detected *in vivo* are related to the alkaline transition or if they represent other structural changes.

DOI: 10.1021/acs.biochem.5b01385
Biochemistry 2016, 55, 407−428

Here we review the biochemical and structural basis for changes in cyt *c* conformation that lead to translocation to different cellular compartments and allow for alternate functions.

Structure, Alternative Conformations, and Folding of Cyt *c*. The three-dimensional structure of horse cyt *c* has been well-characterized (PDB entry 1HRC).[2,42−45] High-resolution crystal structure analysis of horse cyt *c* containing 104 amino acid residues showed that the protein is globular and consists of five helical elements interconnected by Ω loops[46] (Figure 1b). Aside from the loops and helices, horse cyt *c* possesses only two small regions of highly ordered secondary structure, namely, residues 37−40 and 57−59, that form two-stranded antiparallel *β*-sheet interactions supported by three interstrand hydrogen bonds.[2] Overall, the composition of secondary structure elements is very similar to that described in yeast iso-1 cyt *c*[47] and variant G41S of human cyt *c*.[48] An exclusive characteristic of yeast iso-1-cyt *c* is the presence of free Cys102 and a naturally trimethylated Lys72 residue.[49] Also, in contrast with mammalian cyt *c*, yeast iso-cyt *c* exhibits significant differences in surface amino acid residues thought to be important for interactions with other proteins and ligands as well as for folding and holoprotein maturation.

The heme moiety of horse cyt *c* is largely buried within the protein structure, with only 7.5% of its surface accessible to interact with the solvent. The solvent-exposed edge of the heme is surrounded by charged Arg and Lys residues that create a hydrophilic microenvironment. These residues are thought to support interactions with redox partners of cyt *c* and to orient the catalytic center for optimal electron transfer.[50,51]

While the propionate side chains of the heme are protected from solvent exposure, this is somewhat compensated by extensive hydrogen bonding interactions with adjacent polar groups that create a hydrophilic local environment. Analysis of primary sequence shows that amino acid residues involved in heme propionate interactions are highly conserved in eukaryotic cyts *c*.[2] One of these interactions involves one of the two internal structural waters (Wat125, PDB entry 1HRC), which bridges a charge interaction between the carboxyl group of the propionate chain and the guanidinium group of Arg38. The second structural water (Wat112, PDB entry 1HRC) is located close to the heme group. A comparison of oxidized and reduced cyt *c* showed that the position of Wat112 is sensitive to the oxidation state of the metal center.[2] This structural water is 0.9 Å closer to the iron atom in ferric than in ferrous cyt *c*.[2] Alongside shifts in water positioning, the side chains of Asn52 and Tyr67 are markedly sensitive to the oxidation state of the heme in horse, yeast, tuna, and rice cyts *c*.[2] Replacement of Tyr67 with Phe in rat cyt *c* led to an increased stability of the Fe−Met80 bond and increased the pK_a of the alkaline transition by 1.2 units.[14] Further, Tyr67Phe mutant cyt *c* is more resistant to urea denaturation than and equally competent for electron transfer as the wild-type native protein.[14] A consequence of the mutation is the reduced capacity to stabilize the structural water that is held in the cavity via hydrogen bonds from Tyr67, Asn52, and Thr78.[14] Under the optimal prediction that a water molecule can be caged only when at least three H-bonds are formed, the substitution of Tyr67 with Phe could lead to a local increase in heme hydrophobicity.[14] Thus, conservation of Tyr67 may represent an advantage in terms of functional flexibility at the expense of protein stability.[14] These structural water molecules were also identified in the high-resolution structure of yeast iso-1-cyt *c* variant Lys72Ala.[49] Residue Lys72 is trimethylated when iso-1-cyt *c* is expressed in its natural host, and mutation to Ala permitted the elucidation of a buried water channel in the active site that facilitates access to H_2O_2. Variant Lys72Ala exhibits increased peroxidase activity at neutral pH.[49]

A combination of experimental and theoretical studies showed that the redox properties of cyt *c* are controlled by changes in protein dynamics that alter the intramolecular hydrogen bonding network.[52] The high level of conservation of these structural elements across species highlights the importance of hydrogen bonding interactions for cyt *c* function. More broadly, the extensive bonding network of the active site in the family of *c*-type cyts, including the heme−thioeter linkage, is thought to allow large conformational changes without the detrimental effect of heme loss.[12,53] While preservation of respiration is ensured through a highly conserved heme binding pocket, subtle differences in surface amino acid residues are believed to govern the secondary functions of cyt *c*.[54,55] For example, human and yeast cyt *c* have 70% identical amino acids.[47] Major differences between these proteins are found in surface amino acid residues implicated in binding to CL, hydrogen bond formation, and modulation of peroxidase activity.[47] Thus, caution should be used when comparing cyt *c* conformational stability, peroxidase activity, and their role in cellular homeostasis across species.

The overall folding dynamics of cyt *c* follows the pattern observed in proteins without cofactors; however, numerous studies have shown that the heme moiety plays a critical role in cyt *c* folding.[56,57] The heme center adds complexity to the folding process in that it provides a hydrophobic surface and a redox-active metal center for axial ligation. *In silico* models based on the energy landscape theory[58] utilizing the available crystal structure at pH 7 indicate that the folding energy landscapes of cyt *c* are "perfectly funneled" (Figure 3), that is, energetically guided toward the native state and primarily driven by native contacts.[57] These studies also showed that at acidic and alkaline pHs alternative folding pathways exist. For instance, at alkaline pH, Lys residues are deprotonated and compete with Met80 for axial coordination to the heme.[59] It is noteworthy that the pK_a for the alkaline transition (pK_a = 9.1) is ∼1 unit lower than the pH required for deprotonating Lys residues (pK_a = 10.5),[59] unless intramolecular protein bonding interactions facilitate Lys deprotonation at lower pHs. In contrast to native conditions, these alternative folding modes are not perfectly funneled and incorporate distinct structural ensembles because of heterogeneously distributed charged amino acid residues.[57] A major advance in the detection of various conformations within the ensemble has been achieved with single-molecule labeling techniques and the employment of photo-counting histogram (PCH) models.[60] Yeast iso-1-cyt *c* was labeled via its unique free Cys residue with a fluorescent probe that is sensitive to changes in conformation.[60] Measurement of brightness and abundance at different fluorophore:protein labeling ratios and pHs permitted the quantification of individual conformations within the ensemble.[60] Shifting the pH from 7.0 to 9.5 showed the coexistence of two distinct conformational states, and their properties are consistent with the two alkaline conformers, His−Fe−Lys73 and His−Fe−Lys79, previously suggested using standard spectroscopic techniques.[61,62] Further, PCH allowed resolution of the relative abundance of different conformations of cyt *c* while minimizing the effect of the interference of unwanted doubly labeled protein that occurs at high fluorophore:protein ratios.[60]

DOI: 10.1021/acs.biochem.5b01385
Biochemistry 2016, 55, 407−428

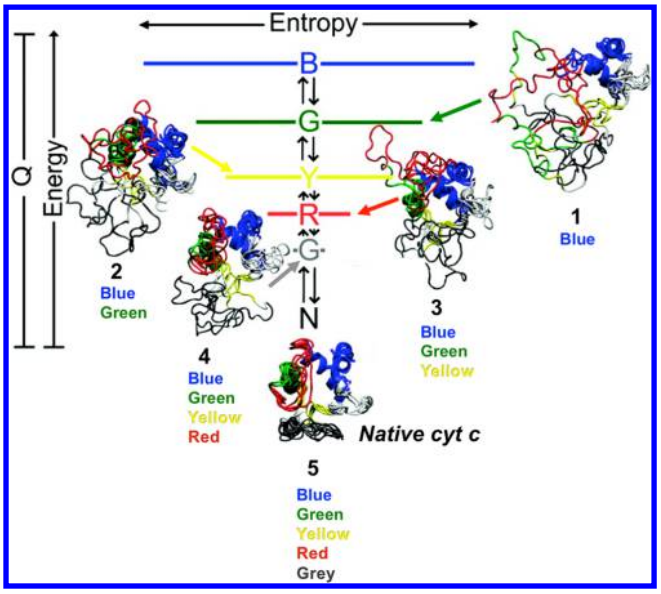

Figure 3. Funneled sequential mechanism of cyt *c* folding. Folding units fold in the following order: blue (residues 95, 96, 98, and 99), green (residue 68), yellow (residues 60 and 64), red (residues 74 and 75), and gray (residues 43, 46, and 52). N depicts the native state. Q represents the reaction coordinate, and the width of each line is proportional to the number of unfolded residues in the ensemble. The configurational entropy is proportional to the number of unfolded residues in each folding state. The first unit to become structured is foldon blue (1). A sequential mechanism comprising intermediate folding states 2−4 leads to fully folded native cyt *c* (5). Modified from ref 57.

Hydrogen exchange measurements under native conditions showed that the folding mechanism of cyt *c* involves five stabilized submolecular folding units or "foldons" that occur in a sequential fashion.[63−67] These discrete foldons fold and unfold dynamically even under native conditions.[66] The first foldon of the sequence comprises helices in the C- and N-termini that exhibit high-density contacts to form a stable structure.[68] The remaining foldons nucleate on the basis of more structured regions that provide greater stability. Mutations and solvent changes that alter the stability of individual foldons cause deviations from the native folding mechanism.[64] Ultrarapid mixing techniques coupled with nuclear magnetic resonance (NMR)-detected hydrogen−deuterium exchange allowed for the observation of hydrogen bond formation during the first 0.14 ms of the folding of horse ferric cyt *c*.[69] A pH dependence study showed that H-bonds of amide chains in the N-terminal helices of cyt *c* exchange substantially during the first 0.1 ms of folding, whereas the C-terminal half of the protein remains protected from H-bond exchange during this time frame. Contacts between C- and N-termini of the protein occur late in the folding process, after 3 ms.[69] The marked variation in the exchange of amide chains in different regions of the protein challenges the proposal that cyt *c* acquires a compact intermediate structure by hydrophobic collapse[70] and supports the notion that the initial phase of folding is a two-state event, involving hydrogen bonding interactions on specific helical elements.[69] Results from this study do not exclude the possibility that faster hydrophobic interactions occur with the heme center in the absence of detectable amide protection. These presumptive clusters of hydrophobic contacts with the heme center might be responsible for the residual structure observed in denatured proteins such as lysozyme[71] and help to explain the blue-shift in the emission spectrum of Trp59 of cyt *c* prior to the main collapse phase of the protein.[72] Likewise, the denaturation pattern of cyt *c* examined by paramagnetic NMR indicates the existence of two stable non-native conformers of the protein.[73] One of the folding intermediates that forms under partially denaturing conditions was attributed to a Lys−Fe−His species, in which one or more Lys residues serve as putative axial ligands.[73] The second conformer was detected under strongly denaturing conditions and its formation was consistent with transition to a bis-His heme species.[73] It has been reported in other studies that the bis-His conformer of cyt *c* represents a kinetic trap in the folding process.[8,74−77] Nonetheless, the ΔG measured by NMR for the formation of the bis-His species is 47 kJ/mol, which is similar to the ΔG for the global unfolding reaction of cyt *c* determined via hydrogen exchange measurements (53.6 kJ/mol).[63] The increasing number of stable conformations of cyt *c* observed during folding, unfolding, and denaturation strengthens the notion that the protein adopts alternative conformations that may be naturally tailored to play roles aside from electron transfer and apoptosis.

The Alkaline Transition at Physiological pH. At neutral pH, the heme moiety in cyt *c* exists in a low-spin configuration, and the iron center is hexacoordinated by the pyrrolic nitrogens of the porphyrin ring and by axial ligands Met80 and His18 of the protein. For many years, it was assumed that the axial ligands remain stably coordinated through the ferrous−ferric redox cycle of cyt *c*. However, numerous spectroscopic studies demonstrated that the coordination geometry of the heme varies with pH, ionic strength, and temperature.[21,78] At elevated pH, ligand exchange reactions occur and involve conformational states of the protein harboring heme in both low- and high-spin configurations as depicted in Figure 4. In the case of

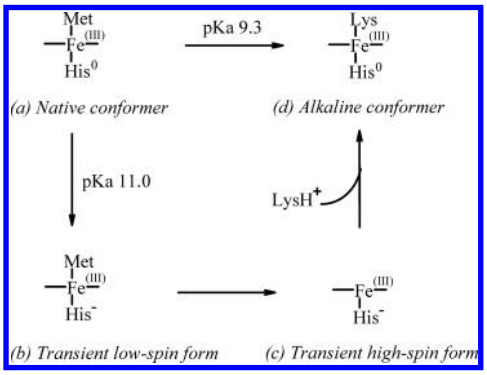

Figure 4. Alkaline transition of cyt *c*. At neutral pH, cyt *c* exists as a hexacoordinated, low-spin heme protein, with His18 and Met80 as the axial ligands of the heme center (a). An increase in pH leads to the deprotonation of the proximal His ligand, weakening of the distal Fe−Met bond with transient formation of species b and c as suggested by spectroscopic methods. Alkaline conformer d arises upon reprotonation of the proximal His ligand and deprotonation of an incoming Lys distal ligand. Adapted from ref 78.

horse cyt *c*, a conformational state that occurs at high pH with a pK_a of ~9.3 termed the "alkaline transition" has been studied in great detail.[19,78,79] Increasing the pH from 1 to 13 gives rise to five distinct conformations of cyt *c*, denominated conformers I−V, going from acid to alkaline pH, respectively.[21] Conformer III occurs at neutral pH, corresponds to the native form of the protein, and possesses a strong absorption band at 695 nm.[21]

DOI: 10.1021/acs.biochem.5b01385
Biochemistry 2016, 55, 407−428

Conversion of conformer III into conformers IV and V is the alkaline transition.

The alkaline transition of cyt *c* is a phenomenon whose functional relevance has been for a long time endured as an "intriguing curiosity".[20] While major progress has been made in studying the alkaline and other alternative conformations of cyt *c*, the functional relevance of these conformers continues to be elusive and intriguing. The observation that the midpoint potential of cyt *c* was affected by pH via a change in protein conformation rather than a change at the heme per se was the second biochemical discovery of that kind, only after the elucidation of the effects of pH on the conformation and catalytic activity of chymotrypsin.[79] Conversion of native ferric cyt *c* to the alkaline form disrupts the axial coordination environment by weakening the Fe−Met bond and allowing substitution with a Lys residue to yield a low-spin, Lys−Fe−His, alkaline conformer of the protein.[79] Results of electron paramagnetic resonance (EPR) and magnetic circular dichroism (MCD) studies suggested that deprotonation of the proximal His residue ($pK_a \sim 11$) acts as a trigger of the alkaline conformation of cyt *c* by weakening the distal Fe−Met bond via the trans effect, and by facilitating the deprotonation of the incoming Lys group.[79] Thus, the alkaline conformer of cyt *c* exhibits a neutral proximal His ligand and a deprotonated Lys residue occupying the distal position.[79]

The alkaline transition of ferric cyt *c* occurs with formation of transient low- and high-spin forms, as depicted in Figure 4. Rapid kinetic measurements coupled to pH jump revealed that the alkaline transition proceeds through the formation of two rate-limiting structural changes that mimic the first two steps in the reversible unfolding pathway of cyt *c*.[80] Further, controlled denaturation and mutagenesis studies showed that the ligand exchange equilibrium that characterizes the alkaline transition is governed by changes in one specific foldon [Ω loop 70−85 (Figure 1)][59] and confirmed Lys73 and Lys 79 as the primary incoming ligands displacing Met80.[81] Resonance Raman (RR) measurements corroborated the role of Lys73 and Lys79 as surrogate axial ligands in the alkaline conformers and suggested that intramolecular contacts between these residues contribute to the conformational transition at the heme pocket.[82] Nonetheless, these findings do not preclude the participation of other axially ligated states during the alkaline transition such as His−Fe−OH and His−Fe−His,[23,83] as will be discussed in the next sections of this review.

To date, only two crystalline structures describing the alkaline conformer of cyt *c*, namely, of yeast iso-1-cyt *c*, obtained at alkaline pH[81] and neutral pH have been elucidated.[84] The alkaline conformer of iso-1-cyt *c* (PDB entry 1NWV) obtained at alkaline pH displays increased mobility compared to the native conformer, with a dramatic collapse of Ω loop 70−85 (Figure 2).[81] With the exception of residue Lys73 coordinating the iron center, no other contacts between Ω loop 70−85 and the rest of the protein could be observed.[81] Indeed, combinatorial analysis of mutants of Lys72 (normally trimethylated under natural conditions), Lys73, and Lys79 in yeast cyt *c* suggests that Ω loop 70−85 is substantially autonomous with respect to the conformational changes that accompany the alkaline transition.[85] This conformational change opened the heme crevice such that approximately 20% of the cofactor is accessible to the solvent.[81] This resulted in greater destabilization of His−Fe−Lys73-ligated cyt *c* by 10 kcal/mol compared to the native conformer.[81] Augmented solvent exposure facilitates the entrance of water-soluble ligands, such as H_2O_2, to prime the peroxidase activity of cyt *c*. Significant changes in other regions of the protein were also observed, as depicted for Ω loop 40−57 (Figure 2g) harboring antigenic region 40−54 in mammalian cyts *c*. Analysis of the alkaline conformer of yeast iso-cyt *c* obtained at neutral pH (PDB entry 4Q5P) revealed that the structure is rather compact, in contrast with its counterpart obtained at alkaline pH.[84] The study showed that a change in axial coordination from Met80 to Lys73 is marked by alterations of the heme binding site that involves hydrogen bond rearrangement and refolding of the heme coordinating loop 70−85 harboring conserved residues Pro76 and Gly77 to form a *β*-hairpin (Figure 2).[84] At neutral pH, the Lys73−Fe alkaline conformer could be observed only in crystalline form.[84] A mimic of this conformer in solution was generated by derivatization of artificially introduced Cys78 with maleimide and showed that the Lys73−Fe alkaline conformer at neutral pH has an increased peroxidase activity.[84] The occurrence of alkaline conformations of cyt *c* at neutral pH underlies the importance of its evolutionarily conserved structural flexibiliy to support noncanonical functions. We posit that this feature of cyt *c* enables functional moonlighting.

A mutant variant Ala81His in yeast iso-1-cyt *c* was employed to simultaneously probe Ω loop 70−85 dynamics by providing a His ligand for the alkaline state near neutral pH and the effect of increasing steric size to mimic the evolutionarily important replacement of Ala in yeast iso-1-cyt *c* to Ile in higher eukaryotes.[86] The study revealed that an increase in steric size at position 81 inhibits rupture of the Fe−Met80 bond.[86] The mutation retarded the alkaline transition by stabilizing the native state without affecting the stability of the alkaline conformer.[86] Interestingly, the stability of the alkaline conformer of variant Ala81His was comparable to that of the alkaline conformers in variants Lys73His and Lys79His, where His73 or His79 serve as the axial ligand upon substitution of Met80.[86] The results also showed that increasing the steric bulk of amino acids at position 81 as observed in higher eukaryotes reduced the opening of the heme crevice required for stable Fe−Met80 bonding, and this structural constraint provides greater control of peroxidase activity.[86] Several studies have independently shown that structural changes such as mutations or post-translational modifications facilitate the transition to alternative conformers of cyt *c* at neutral pH, which has important implications in terms of biological function. Also, the predominance of alternative conformations seems to vary across species.[55] While yeast iso-1-cyt *c* exhibits a significant population of intermediate conformational states under native conditions, human cyt *c* requires the presence of additional factors to trigger conformational transitions and peroxidase activity, such as CL binding and post-translational modifications.[55] Furthermore, even within species, the conformational changes associated with the usage of Lys73 versus Lys79 as the incoming axial ligand in the alkaline transition are significantly different, yet both occur under physiological conditions. This implies that different triggers may exist, leading to different alkaline conformers in response to cellular needs. Identifying the nature and mechanism of action of those triggers is warranted in the coming years.

Cardiolipin and Phospholipid-Induced Conformational Changes. Cytochrome *c* displays a high affinity for acidic phospholipids, a feature allowing its association with the inner mitochondrial membrane.[87] The interaction of cyt *c* with authentic and *in vitro* models of the mitochondrial membrane is

DOI: 10.1021/acs.biochem.5b01385
Biochemistry 2016, 55, 407−428

influenced by ionic strength, pH,[15,88,89] and the composition of acidic phospholipids.[90−92] Three discrete sites have been described for the interaction of cyt *c* with lipidic structures, namely, sites A, C, and L[93] (Figure 5). In general, the structural

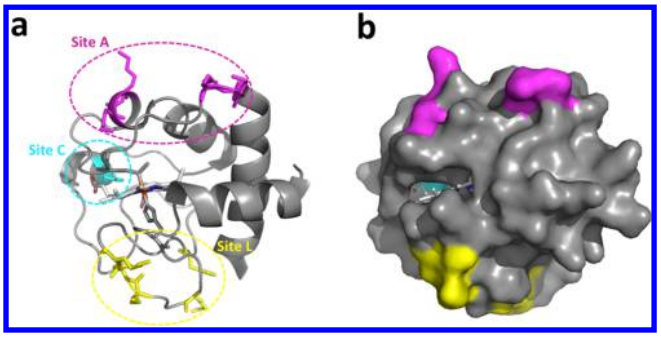

Figure 5. Phospholipid binding sites in horse cyt *c*. (a) Cartoon representation of horse cyt *c* (PDB entry 1HRC) depicting phospholipid binding sites A, C, and L. Site A (magenta) comprises residues Lys72, Lys73, Lys86, and Lys87; site C (cyan) consists of key amino acid residue Asn52, and site L (yellow) incorporates amino acid residues Lys22, Lys25, Lys27, His26, and His33. Sites A and L interact with lipid structures mainly via electrostatic interactions, whereas site C does so through hydrogen bonding contacts. (b) Surface map representation of horse cyt *c* illustrating solvent accessibility and geometry of the phospholipid binding sites.

determinants that support cyt *c*−phospholipid interactions are (a) the presence of negatively charged groups that could interact with positively charged surface Lys residues in cyt *c* and (b) a nonpolar structure to access the hydrophobic active site of cyt *c*.[94,95] It has been postulated that cyt *c* interacts with phospholipids via a general mechanism known as "extended-lipid anchorage" whereby one of the phospholipid acyl chains juts out of the biological membrane and intrudes into a hydrophobic channel in cyt *c*.[25] The other acyl chain of the phospholipid remains anchored in the bilayer, bridging the protein−membrane association. cyt *c* binds to deprotonated phosphatidylglycerol (PG) via site A by means of electrostatic interactions, and this is reversed by ATP; on the other hand, binding to protonated PG occurs at site C, in a manner independent of ATP, and involves hydrogen bonds.[96] Apart from sites A and C, cyt *c* possesses one more site, known as site L, which has a preference for acidic phospholipids and is markedly sensitive to pH.[15] Electrostatic interactions with site A involve amino acid residues Lys72, Lys73, Lys86, and Lys87, whereas site C operates via hydrogen bonding with residue Asn52.[94] Lipid interactions with site L are governed by electrostatic interactions with residues Lys22, Lys25, Lys27, His26, and His33 with a pK_a of ~7.0[15,94] (Figure 5). The amino acid composition of site L and the observed sensitivity to pH suggested that interactions at this site could be influenced heavily by acidification of the mitochondrial intermembrane space, an event that occurs naturally upon transport of protons coupled to electron transfer in the respiratory chain.

The association of cyt *c* with phospholipids leads to conformational changes that affect its function. One of the most remarkable examples is the association of cyt *c* with CL, a phospholipid that is specifically found in the inner mitochondrial membrane and in the cellular membranes of prokaryotes.

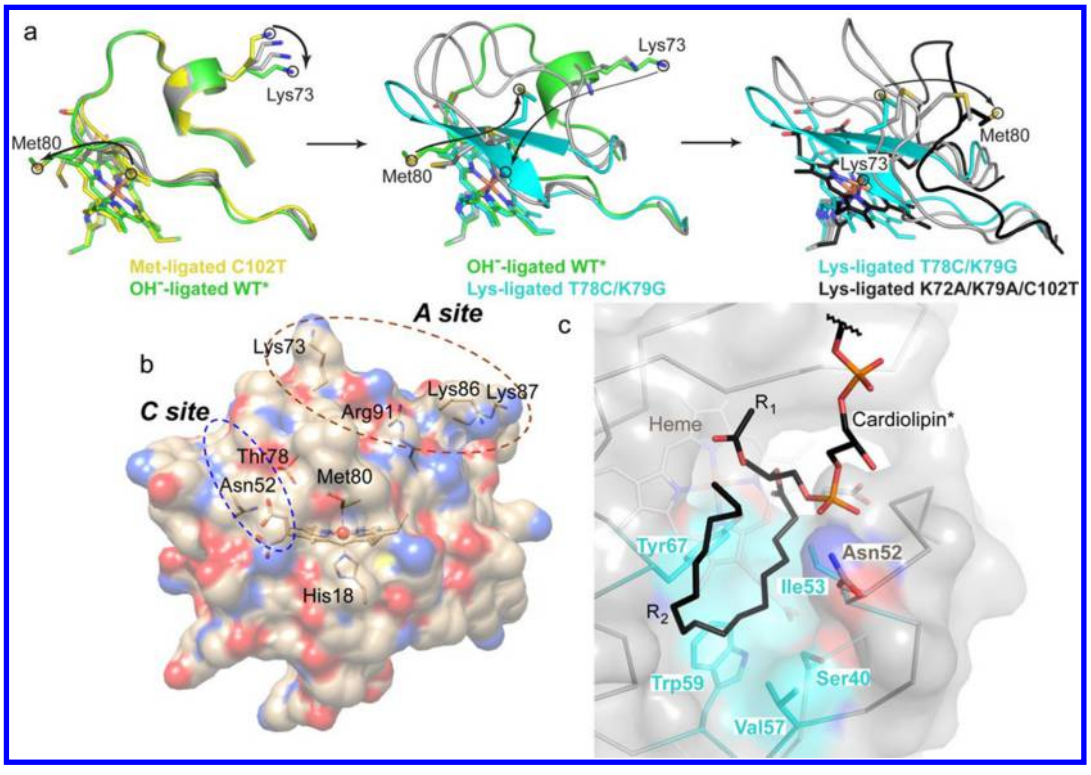

Figure 6. Structural transition from Met80−Fe to Lys73−Fe in cyt *c* and its impact on CL binding. (a) A model for the transition from Met- to Lys-bound heme was built using mutants that represent several intermediate conformers, including a hydroxide-bound heme. The global conformational changes that accompany the initial and final ligated states are shown with arrows. (b) Proposed CL binding sites A and C are shown with dotted circles. Critical surface residues required for hydrogen bonding and acyl insertion are indicated. (c) A suggested CL binding pocket based on positive electron density in the $F_o - F_c$ map was generated using Coot. Reproduced from ref 84. Copyright 2015 American Chemical Society.

DOI: 10.1021/acs.biochem.5b01385
Biochemistry 2016, 55, 407−428

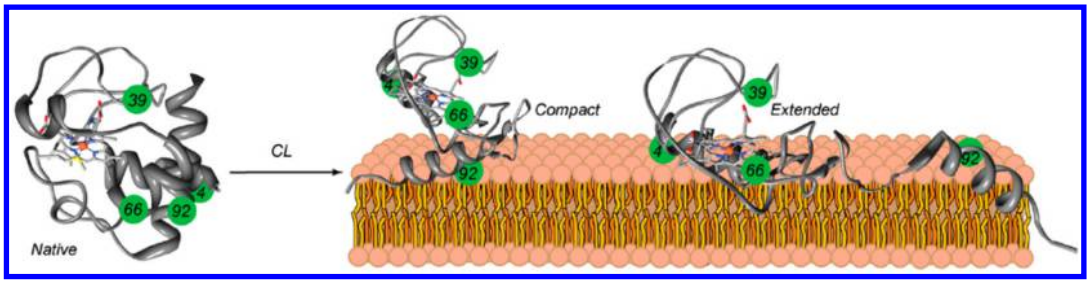

Figure 7. Alternative conformations of cyt *c* bound to cardiolipin. The reversible association of cyt *c* with CL has been probed via single-labeling techniques. Fluorescent dyes placed in each of four highly flexible folding units (positions 4, 39, 66, and 92) reported on conformational changes that occur upon binding to CL. In the presence of CL, cyt *c* undergoes the transition from the native state to two alternative conformers that differ in their degrees of compactness. The cyt *c*−CL complex is sensitive to high ionic strength and oxidation of CL, leading to dissociation from the lipid structure. Reproduced from ref 112. Copyright 2012 National Academy of Sciences.

Binding of CL to cyt *c* has dual effects. CL anchors cyt *c* to the membrane to enable electron transfer in the respiratory chain; however, it can also switch cyt *c* into a peroxidase, and the subsequent oxidation of CL by this activity, together with the translocation of oxidized CL from the inner to the outer mitochondrial membrane, mediates the induction of apoptosis.[97] The general association of cyt *c* with mitochondrial membranes and a role for lipoperoxidation in this process were introduced more than two decades ago,[98−100] yet the molecular basis for the partition of cyt *c*−CL between respiration and other routes such as apoptosis remains unresolved. Cardiolipin binds to cyt *c* such that its two aliphatic side chains interact with sites A and C. Cyt *c*−CL interactions at site A are displaced by ATP and involve electrostatic interactions with residues Lys72, Lys78, and Lys86.[89,91] Site C involves a hydrophobic cleft that intrudes from the surface into the heme crevice of cyt *c*. Within this site, the second acyl side chain of protonated CL is stabilized via H-bonding interactions with Asn52 with the concomitant breakage of the H-bond between adjacent residues His26 and Pro44.[101] Placement of CL into site C changes the conformation of cyt *c* into an alternative, more open state that disrupts Fe−Met80 coordination, enhancing peroxidase activity.[101,102] The crystal structure of the alkaline Lys73−Fe−His18 conformer of yeast iso-cyt *c* obtained at neutral pH indicated that the transition of Fe−Met80 to Fe−Lys73 led to an increase in the volume of the heme pocket that would alow insertion of an acyl moiety of CL interacting with residue Asn52 (Figure 6).[84] This is consistent with the extended-lipid anchorage proposal.[25]

However, evidence exists that loss of Fe−Met80 axial ligation alone is not sufficient to account for the CL-dependent increase in peroxidase activity.[103,104] A more complex mechanism has been postulated whereby peroxidation and subsequent dissociation of CL precede the release of cyt *c* from mitochondria in response to an apoptotic stimulus.[22] Indeed, no peroxidation of CL could be detected in cyt *c*-knockout cells,[22] and cells deficient in CL are resistant to apoptotic stimuli.[105] Peroxidation of CL leads to a transient increase in the amount of free cyt *c* available in the intermembrane space, favoring its translocation across the outer mitochondrial membrane during apoptosis. Further, time-resolved experiments demonstrated that CL peroxidation precedes the release of cyt *c* and caspase activation.[22,103] A study conducted with the natural variant G41S of human and mouse cyt *c* showed that mutation of Gly41 to Ser, Ala, or Thr increased the peroxidase activity of native free cyt *c*, but not that of CL-bound cyt *c*.[31] The study identified no differences between the extent and rates of release of native versus Gly41 variants of cyt *c* from mitochondria under conditions that stimulate apoptosis.[31] A possible explanation for this effect is that binding to CL perturbs the conformation of loop 40−57 in cyt *c*, which could be the dominant pathway at work for enhancing peroxidase activity.[106,107]

Mechanistic studies have shed light on the specific sites in cyt *c* that are responsible for the peroxidation of CL. Site-directed mutagenesis of each of the four Tyr residues present in horse cyt *c* and comprehensive biophysical analysis of individual mutant proteins led to the conclusion that Tyr67 is the primary site for CL and other lipid oxygenation, being superior to the other Tyr residues.[11] The role of tyrosyl radicals in the peroxidation of lipids is well-established.[108,109] The cyt *c*−CL ensemble is very heterogeneous in nature,[110,111] hampering characterization by means of traditional structural biology approaches. To overcome this hurdle, one study utilized time-resolved fluorescence resonance energy transfer (FRET) measurements to investigate the folding states of cyt *c* bound to CL using a dansyl probe placed at artificially introduced Cys residues at positions 4, 39, 66, and 92 of horse cyt *c*.[112] These positions lie in four regions of the protein that exhibit distinct stability.[65] The dansyl moieties (donors) are quenched by FRET to the heme center (acceptor) in cyt *c*. The study showed that the peroxidase activity of cyt *c* increases with CL-induced conformational changes to a more extended, open structure at different ionic strengths.[112] Addition of CL increased the dansyl fluorescence intensity for all individually labeled variants. On average, the predominant conformational state of cyt *c* bound to CL is looser than in the native structure but more compact than in fully denatured cyt *c* (Figure 7). The largest shifts in fluorescence wavelength maxima were seen for individually labeled variants at positions 66 and 92, suggesting a more hydrophobic environment.[112] A high salt concentration weakened the interaction of positively charged cyt *c* with negatively charged CL, culminating in the dissociation of the protein from CL-containing liposomes.[112] At high salt concentrations, the composition of the ensemble shifted toward more compact, nativelike conformations. Populations of extended conformations of cyt *c* were observed for variants of residues 92 and 4, located at the C- and N-termini, respectively.[112] Residue 92 is close to phospholipid binding site A of cyt *c*. Therefore, the structural loosening upon CL binding further confirms the marked affinity of site A for anionic phospholipids.[90,91]

The presence of extended structures in regions comprising target residues 4 and 92 implies that stabilizing bonding

DOI: 10.1021/acs.biochem.5b01385
Biochemistry 2016, 55, 407−428

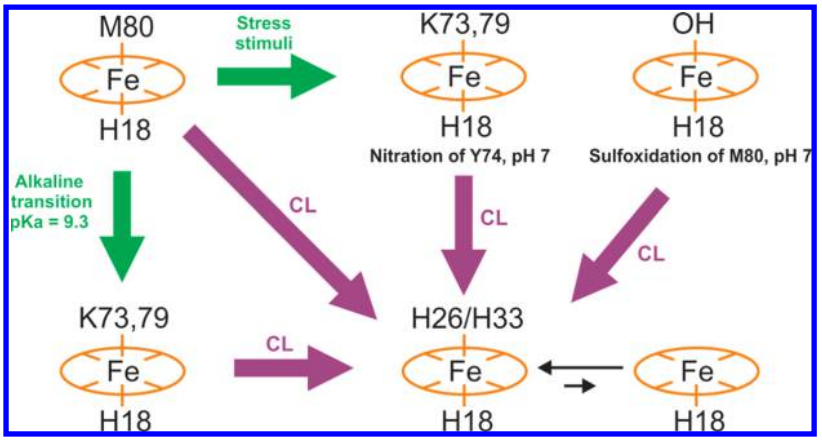

Figure 8. Cytochrome *c*—cardiolipin interactions. Different axial coordination conformers of cyt *c* can be produced by alkalinization, tyrosine nitration, or methionine sulfoxidation. Upon binding to CL-containing liposomes, all conformations converge to a spectrally common bis-His form that presents high peroxidase activity and is in equilibrium with small amounts of pentacoordinated species.

interactions between N- and C-termini helices have been disrupted for some of the protein conformers, leading to the formation of extended and open structures in the ensemble. An important region that underwent extension is that of target residue 39. This suggests unfolding next to Pro44[36] and agrees with structural rearrangement of the loop region comprising residues 37−61.[113] Of note, region 40−54 of conformationally altered cyt *c* (see below) displays antigenicity recognized by a mAb (1D3),[36] which provides a unique opportunity to detect CL-induced alternative conformations of cyt *c* at the cellular level. In summary, these studies demonstrated the existence of compact and extended conformations of cyt *c*, which are triggered by CL binding and factors affecting cyt *c*−CL interactions such as ionic strength.[112]

In line with these findings, an examination of the surface interactions of cyt *c* with CL-containing liposomes revealed two distinct binding sites on the protein that cause different extents of unfolding.[114] The results showed the coexistence of two distinct conformations of ferric cyt *c*, namely, one that resembles the native structure and a second, partially unfolded non-native conformation.[114] Site 1 is unaffected by ionic strength, whereas site 2 exhibits a greater population of protein in the native state in the presence of NaCl. The latter site likely reflects an equilibrium of highly unfolded proteins bound via electrostatic interactions and less unfolded proteins supported by H-bonding interactions with Lys side chains or hydrophobic contacts.[114] Importantly, sites 1 and 2 in this work do not represent site A, C, or L previously discussed herein, but instead a new two-binding site model to describe the interactions of cyt *c* with CL. Site 1 is a high-affinity site postulated to support the nativelike state of cyt *c* that is suitable for electron transfer in the inner mitochondrial membrane.[114] Binding site 2 represents a conformation of cyt *c* bound to CL in which the axial Fe−Met80 bond is disrupted impeding electron transfer reactions for cellular respiration.[114] Binding of CL to cyt *c* may occur at different sites and exhibit distinct effects. For example, results from one NMR study utilizing reverse micelle encapsulation described an additional CL binding site in cyt *c*, denominated site "N", that does not overlap with previously described sites A, C, and L.[115] In contrast to the results obtained by several groups, these studies documented no effect of CL binding on cyt *c* conformation and no signs of protein unfolding.[115] These findings agree well with a multidimensional magic angle spinning (MAS) solid-state NMR study that examined the interaction of uniformly ^{13}C- and ^{15}N-labeled horse cyt *c* with CL-containing lipid bilayers.[116] Results from this study showed that binding of cyt *c* to membranes led to an increase in peroxidase activity but was without effect on protein conformation or membrane penetration.[116] Under these experimental conditions, cyt *c* interacts with CL at the membrane−cytoplasm interface, where it undergoes an increase in peroxidase activity but without significant unfolding.[116]

Interpretation of these contrasting findings is limited by the use of different model systems that aim to mimic the mitochondrial compartment. In the absence of crystal structures of CL-bound cyt *c*, the precise site of CL binding shall remain open to further investigation.

Native and Alternative Conformations of Cyt *c* Converge to Bis-histidine Ligation upon Binding of CL. The multiple spectroscopic studies reported for complexes of cyt *c* with CL and other model systems do not afford a uniform picture of the partition of cyt *c* between electron transfer and peroxidatic activities. For example, RR spectroscopy reveals that the interactions of cyt *c* with DOPG vesicles induce the formation of alternative hexa- and pentacoordinated species such as His/His, H_2O/His, and Fe-His, depending on the relative protein/lipid concentration.[117] For cyt *c*−SDS complexes, the main axial coordination has been determined as His/His by means of NMR spectroscopy.[118] MCD studies of cyt *c*−CL complexes, on the other hand, suggest that the coordination of the ferric protein at neutral pH is Lys/His and OH^-/His,[83] while RR studies on similar systems suggest the coexistence of Lys/His and pentacoordinated Fe−His species.[119]

The coordination of cyt *c* in complexes with unilamellar and multilammelar CL liposomes has been recently revisited employing RR and UV−vis spectroscopies.[23] The studies comprise the WT protein, double and triple mutants, and variants with specific post-translational modifications such as Met80 oxidation and mononitration at tyrosines 74 and 97. The different variants have the peculiarity of stabilizing (or preventing) different axial coordinations such as Met/His, Lys/His, OH^-/His, and pentacoordinated Fe−His and, therefore, constitute a valuable toolbox for obtaining reliable spectral components. On the basis of these studies, it is possible to conclude that the interaction of native (Met/His) cyt *c* with CL liposomes leads to a His/His axial coordination as the main

DOI: 10.1021/acs.biochem.5b01385
Biochemistry 2016, 55, 407−428

spectral component in the complexes.[23] Moreover, cyt *c* variants with alternative coordinations, particularly OH^-/His and Lys/His, exhibit similar behavior, indicating that all the alternative conformations tend to converge to a common His/His axial ligation upon binding of CL (Figure 8).[23]

Role of CL on the Intracellular Transit of Cyt *c*. A fluorescence correlation spectroscopy (FCS) study of the effect of CL on the peroxidase activity of yeast and human cyts *c* identified two important components of the conformational event: (a) a transition from a close, compact structure to a more open, extended conformation of the active site under native conditions and (b) the formation of oligomers induced by CL.[55] The peroxidase activity correlated well with a predominance of an open state under native conditions, which preceded the formation of oligomers. The data showed substantial formation of oligomers in yeast iso-cyt *c* upon interaction with CL, whereas the contribution of CL to oligomer formation in human cyt *c* was very small.[55] It was concluded that oligomer formation plays a major role in the peroxidase activity of yeast iso-cyt *c*, and the effect was ascribed to subtle differences in surface amino acid residues that dictate different outcomes upon CL binding in this organism.[55]

Despite organism-specific differences, it is clear that the interaction of CL with cyt *c* changes its conformation. In a recent study, it was proposed that this event may aid in the translocation of cyt *c* across the inner mitochondrial membrane.[120] Cytochrome *c* interacted strongly with CL embedded in membrane vesicles, and this was accompanied by bursts of leakage of cyt *c* through the lipid structure.[120] Recruitment of cyt *c* by CL in the vesicles was followed by leakage of cyt *c* across the membrane over a period of 1−2 min.[120] Imaging analysis showed that cyt *c* translocated through newly formed pores that remained open to all molecules of a certain cutoff size and eventually closed, indicating the reversibility of pore formation.[120] The addition of ATP reduced the rate and extent of cyt *c* translocation, suggesting a competitive process and/or weaker cyt *c*−CL interactions at high ATP concentrations.[120] Further, in another study, it was shown that the peroxidase activity of CL-bound cyt *c* stimulated leakage of chemical probes carboxyfluorescein, sulforhodamine B, and 3 kDa fluoresent dextran from liposomes.[121] This leakage exhibited selectivity toward the pore size, as 10 kDa fluorescent dextran was unable to cross the liposomal membrane.[121]

Altogether, the knowledge accumulated thus far indicates that alternative conformations of cyt *c* that arise via the interaction with CL might be essential for membrane permeation and subsequent translocation of this and other proteins for downstream cellular signaling in the cytosol and other compartments.

Indeed, a new route for intracellular trafficking of cyt *c*, namely, the translocation of cyt *c* into the nucleus in response to DNA damage, has been observed.[122] Transit of cyt *c* from the mitochondrion to the nucleus was not initiated by stimulation of the death receptor or stress-induced pathways. Once in the nucleolus, cyt *c* blocked histone chaperones SET/TAF-Iβ impeding nucleosome assembly. In doing so, cyt *c* performs a dual function by triggering apoptosis and by blocking cell survival at the fundamental level of DNA biosynthesis.[122]The protein conformation, the presumptive role of phospholipid interactions, and the mechanism of entrance of cyt *c* into the nucleus remain to be established.

Post-translational Modifications That Alter Cyt *c* Structure and Function. Among the better studied post-translational modifications (Table 1), the nitration of cyt *c* by peroxynitrite and other nitric oxide-derived oxidants has received an increasing amount of attention, largely because of its potential role in human diseases accompanied by oxidative stress.[29,123] Of the four conserved Tyr residues of human cyt *c*, Tyr74 and Tyr97 are exposed to the solvent whereas Tyr67 and Tyr48 are buried within the protein matrix (Figure 9). Mono- and dinitrated variants of cyt *c* can be prepared *in vitro* using slow fluxes of peroxynitrite near physiological conditions and purified to homogeneity (Figure 10).[123,124] Nitration of Tyr residues occurs *in vivo* and alters the functions of proteins.[125−127] Endogenously formed nitrated cyt *c* has been detected in cultured cells and in disease models characterized by nitroxidative stress.[128−130] In terms of function, nitration of cyt *c* impairs its ability to activate caspase-9, a crucial step in apoptosis.[131,132] Nitration of Tyr residues reduces the pK_a of the phenolic -OH group by approximately 3 units and incorporates a steric bulk of 45 Da (Figure 9a,b). Nitration of individual Tyr residues destabilizes the axial Fe−Met80 bond, facilitating the alkaline transition to form alternative conformers of cyt *c*. This change in heme configuration leads to a reduction of its midpoint potential, impeding electron transfer in the mitochondrial respiratory chain.[29,133,134] Indeed, mononitrated and mono-Tyr mutants of cyt *c* exhibit a midpoint potential lower than that of the native counterpart.[135] Physicochemical studies have shown that perturbations of the heme environment due to Tyr nitration and local electric fields operate by distinct mechanisms.[135] Studies of the role of nitro groups in 3-NO_2-Tyr residues in terms of bonding interactions have led to some controversy in the field. Individual nitration of solvent-exposed Tyr74 resulted in a more facile, early alkaline transition, with a pK_a value of 7.1.[30] cyt *c* nitrated in position Tyr74 adopted the alkaline conformation at neutral pH with the expected rupture of Fe−Met80 axial ligation and substitution of a Lys residue to form a low-spin hexacoordinated complex.[30] Mutation of Tyr residues to Phe was employed to probe the effect of nitration and bonding interactions in the relevant Ω loops in the alternative conformations of nitrated cyt *c*. Results of the study indicated that nitration of Tyr74 influences heme geometry by steric perturbation of highly flexible Ω loop 70−85, an effect that is conveyed to the heme center via Tyr67 located in the vicinity.[30] Replacement of Tyr67 with Phe increased the pK_a of the alkaline transition to 11, which antagonized the effect of nitration at Tyr74, i.e., induction of an early alkaline transition. This supports the postulate that a hydrogen bond interaction between Tyr67 and the sulfur atom of Met80 mediates the observed long-range effect via a conformationally contiguous Tyr74-Glu66-Tyr67-Met80-Fe network.[30] Tyr67 is the only residue restricted within a helical structure, in the proximity of the heme site, unlike the remaining tyrosine residues that are all located in flexible Ω loops (Figure 9c,d). Substitution of Tyr67 with Arg in human cyt *c* led to rupture of the Fe−Met80 bond, weak distal ligation by Arg, and an 8-fold increase in peroxidase activity,[136] a behavior comparable to that of the Tyr67Arg variant of yeast iso-cyt *c*.[137] In contrast, substitution of Tyr67 with His in human cyt *c* was without effect on peroxidase activity or Fe−Met80 ligation,[136] whereas the yeast counterpart exhibited an increased peroxidase activity.[137] This suggests that subtle structural differences in the H-bond network of these cyt

DOI: 10.1021/acs.biochem.5b01385
Biochemistry 2016, 55, 407−428

Table 1. Chemical Modifications That Alter Cyt *c* Function

chemical modification	organism	effect	refs
Ala81His	yeast	alkaline conformer less stable than native conformer	86
Lys79His	yeast	alkaline conformer more stable than native conformer	86
acetylation of Lys	mouse	reduction in positive charge	145, 146
		increased hydrophobicity	
		lengthening of the side chain, steric effects	
trimethylLys72Ala	yeast	disrupted Fe−Met80 axial bond	49
		higher peroxidase activity	
Gly41Ser	human	increased level of apoptosis	28, 48, 142, 143
		increased spin density on pyrrole ring C and a faster electron self-exchange rate	
		higher peroxidase activity	
		stabilization of protein radicals	
Tyr48His	human	increased level of apoptosis	32
		decreased level of respiration	
Tyr48His	yeast	lower heme midpoint potential (~80 mV)	33
Gly41Ser	human	higher peroxidase activity compared to that of native cyt *c*	31
Gly41Thr	mouse	no changes in peroxidase activity compared to that of cyt *c* bound to cardiolipin	
Gly41Ala			
nitration of Tyr46	human	rearrangement of H-bond network	140, 194
		high-spin heme	
		facile alkaline transition	
		defective apoptosome	
		protein degradation	
nitration of Tyr48	human	rearrangement of H-bond network	140, 194
		high-spin heme	
		facile alkaline transition	
		defective apoptosome	
		degradation	
nitration of Tyr74	human	increased peroxidase activity	138
		disrupted interaction with caspase-9, inhibition of apoptosis	
nitration of Tyr74	horse	lower pK_a for alkaline transition	157
		lower midpoint potential	
		deprotonation of Tyr74	
		high peroxidase activity	
phosphomimetic Tyr48-Glu	human	lower heme midpoint potential (~80 mV)	141
		lower pK_a alkaline transition	
		disrupted Apaf-1-mediated caspase activation	
		disrupted interaction with cardiolipin	
phosphomimetic Tyr97-Glu	human	less stable than native protein	141
individual nitration of Tyr46, Tyr48, Tyr67, Tyr74, and Tyr97	human	lower midpoint potential	134, 135
		nitration effects are additive	
		lower affinity for Apaf-1	
		disrupted caspase activation	
sulfoxidation of Met80	horse	high-spin heme	144
		high peroxidase activity	

c variants have a profound impact in their reactivity toward hydrogen peroxide.[137]

A structural study performed with yeast iso-1-cyt *c* provided evidence that the geometry of Tyr67 near the iron center is such that it could serve as a weak axial ligand replacing Met80 in the alkaline conformer.[81] Molecular dynamics calculations performed on mamalian cyt *c* found no evidence of H-bonding between residue Tyr67 and axial ligand Met80 but suggested instead the presence of a hydrogen bond between Tyr67 and Thr78, the latter residue belonging in the same foldon.[138] A more recent combined experimental and computational study that, in contrast to the previous one, implemented optimized parameters for H-bonds with a S atom as acceptor revealed the existence of a weak Tyr67−Met80 H-bond that modulates electron transfer kinetics trough flexible Ω loops 20−30 and 70−87.[139] Foldon Ω loop 70−85 was also shown to be the major contributor to the ligand exchange reaction that accompanies the alkaline transition.[59] While the dynamics of H-bond formation via residue Tyr67 may be promiscuous in nature, consensus about the importance of far-reaching effects in controlling heme electronics and, therefore, the peroxidase activity of cyt *c* exists. Individual, successive replacement of Tyr with Phe leads to additive effects in reducing the midpoint potential of cyt *c*, even though no correlation could be established between the previously reported values of peroxidase activity[123,138] and the relative contribution of each non-native coordination state.[135] This lack of correlation is not surprising per se, as RR measurements do not report on the conformational changes that accompany the different coordination states within the alkaline ensemble. Nonetheless, an important conclusion from these spectroscopic studies is that modification of Tyr74 and Tyr67 is detrimental to the activity of cyt *c* in both cellular respiration and apoptosis, through a molecular mechanism whereby nitration precipitates the alkaline transition and the formation of alternative conformers.

This proposal was substantiated by the finding that a conformer of cyt *c* in which the Fe−Met80 bond was disrupted by substitution of Met80 with Ala had increased peroxidase activity and translocated spontaneously from mitochondria to the cytoplasm and nucleolus in the absence of apoptosis.[24] The release of Met80Ala cyt *c* from mitochondria was dependent on peroxidase activity, with oxidation targets that are yet to be identified.[24] High-spin variants not seen in nitrated cyt *c* were also observed, and these exhibited the highest peroxidase activity and were reactive with mAb 1D3.[24] Because nitrated wild-type cyt *c* also undergoes translocation to extramitochondrial compartments, variant Met80Ala represents one model of endogenously formed alternative conformations of cyt *c*. In a separate study, individual nitration of residues Tyr46 and Tyr48 of human cyt *c* induced the specific degradation of the protein upon its transition to a high-spin state.[140] Thus, nitration of specific Tyr residues leading to a variety of alternative conformations of cyt *c* may be exploited *in vivo* to elicit select cellular responses, creating an additional layer of functional diversity.

Apart from nitration, cyt *c* is also a target for phosphorylation of its Tyr residues, especially at sites Tyr48 and Tyr97.[141] Biophysical characterization of phosphomimetic mutants Tyr48Glu and Tyr97Glu suggested that phosphorylation at these sites may be a physiologically relevant process. Mutant cyt *c* Tyr97 exhibited stability significantly lower than that of the native protein, whereas Tyr48Glu displayed an even more interesting phenotype characterized by a lower pK_a for the

DOI: 10.1021/acs.biochem.5b01385
Biochemistry 2016, 55, 407−428

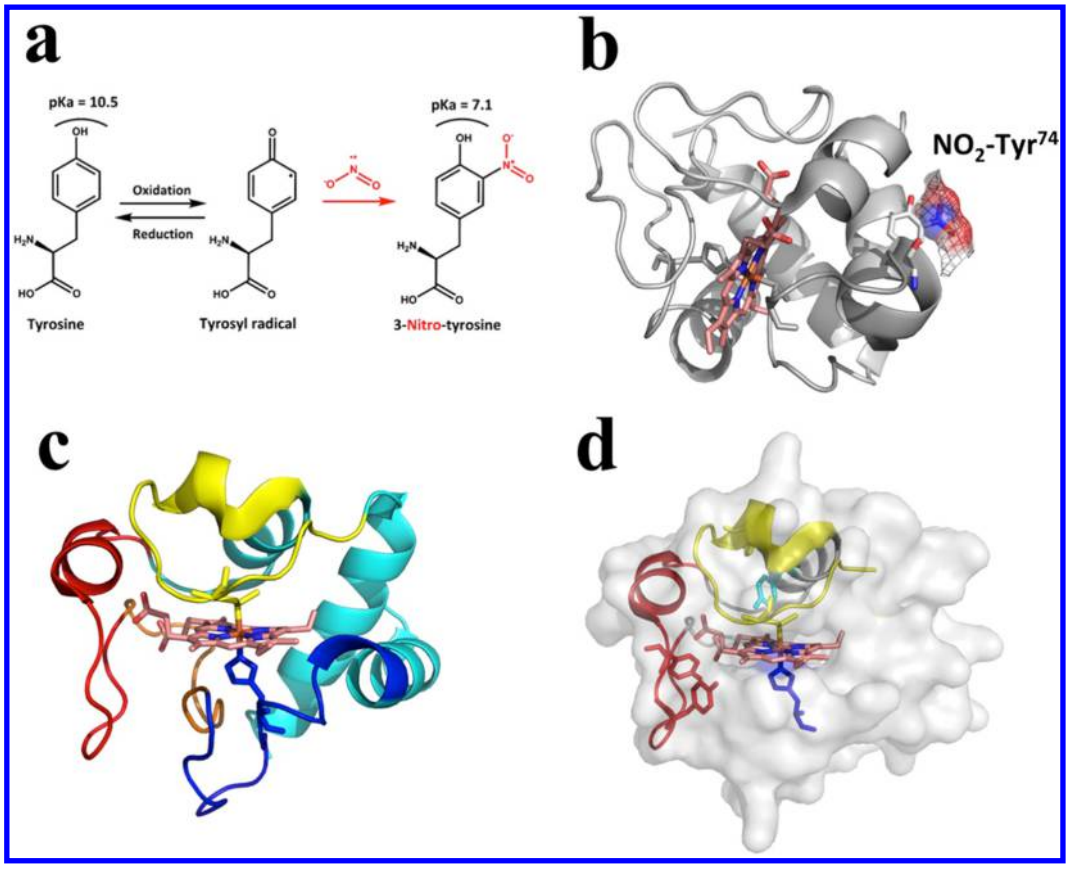

Figure 9. Reaction and substrates of nitration in cyt *c*. (a) Tyrosine residues are present in 3−4% abundance in both buried and solvent-exposed areas of proteins. Deprotonation of the alcohol has a pK_a of 10.5. Tyrosine oxidation to tyrosyl radical and subsequent reaction with $^{\bullet}NO_2$ to produce 3-nitrotyrosine increases the acidity of the phenolic group, rendering it more prone to deprotonation under physiological conditions (pK_a = 7.1). (b) Representation of human cyt *c* variant G41S (PDB entry 3NWV) nitrated at residue Tyr74. The nitro group is shown as spheres. A mesh representation of the surface highlights the steric bulk associated with the conversion of Tyr74 to NO_2Tyr74. (c) Spatial arrangement of flexible Ω loops (blue for residues 12−28, orange for residues 29−40, red for residues 41−57, and yellow for residues 70−85) in human cyt *c* variant G41S. (d) Topology of tyrosine residues shown within a surface representation of human cyt *c*. Tyr46 and Tyr48 contained in loop 41−57 are shown as red sticks. Tyr 74 within loop 70−85 is shown as yellows sticks. Tyr67, which does not belong in any of the flexible loops, is represented as cyan sticks.

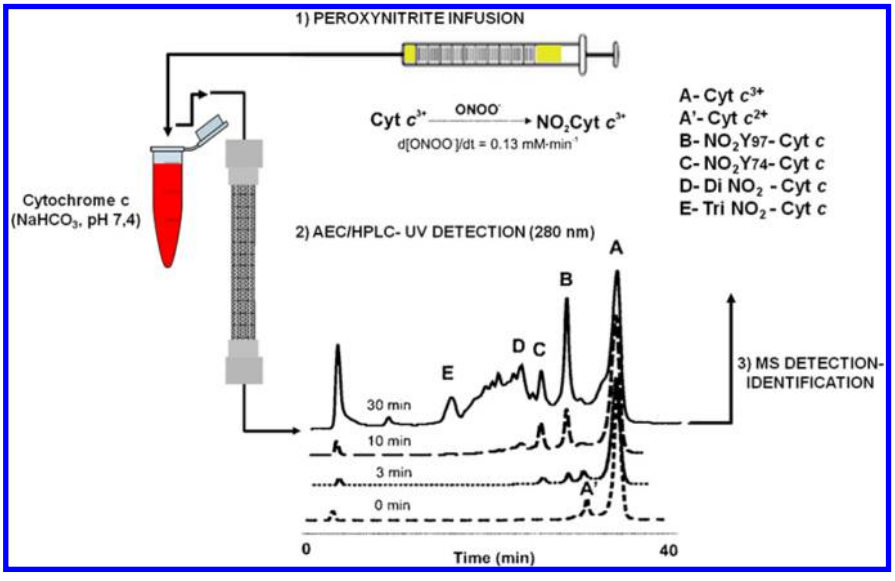

Figure 10. Preparation of nitrocyt *c*. Slow fluxes of peroxynitrite lead to the time-dependent formation of mono-, di-, and polynitrated variants of cyt *c*. Each form can be isolated and characterized individually by anion exchange chromatography (AEC)/HPLC and mass spectrometry. Residues Tyr74 and Tyr97 are the preferred targets of nitration under these experimental conditions, suggesting that reaction selectivity is strongly influenced by solvent accessibility. Adapted from ref 123.

DOI: 10.1021/acs.biochem.5b01385
Biochemistry 2016, 55, 407−428

Table 2. Redox Midpoint Potential and Peroxidase Activities of the Different Axial Coordination Conformers

axial coordination	Met/His	Lys/His	OH^-/His	His/His	H_2O/His[c]
protein variant		NO_2-Cyt74[157]	SO-Cyt[144]	cyt *c*−CL[23]	
$E°$ (mV)	261[162]	−100 to −200[157,195]	135[144]	−80 to −143[83,162]	<−150
relative peroxidase activity	1	7[157]	7−10[144]	5−300[22,23,106]	50−1000[23,158]

alkaline transition, a reduced midpoint redox potential, and an antagonistic behavior toward Apaf-1-mediated caspase activation, a crucial event for apoptosis.[141] On the basis of these findings, the authors postulated that cyt *c* naturally phosphorylated at position Tyr48 may act as an anti-apoptotic switch *in vivo*.[141] It is noteworthy that phosphorylation occurs at Tyr residues that are less preferred substrates for nitration, allowing both mechanisms to coexist under physiological conditions.

Additional studies continue to emerge showing that other naturally occurring modifications of cyt *c* such as mutant Gly41Ser in humans,[28,48,142,143] sulfoxidation of Met80 in horse,[144] and the acetylation of Lys residues as observed in murine cyt *c*[145,146] modulate the peroxidase activity, charge, and hydrophobicity of cyt *c*. This, in turn, could conceivably alter the capacity of cyt *c* to sense and respond to environmental signals, including those associated with cellular compartmentalization, allowing new functions.

Zwitterionic Lipids Activate Specific Sulfoxidation of Met80 by Hydrogen Peroxide. In addition to CL, mitochondrial membranes are rich in zwitterionic phospholipids such as phosphatidylcholine (PC) and phophatidylethanolamine (PE), which comprise >70% of the total lipid content and have a quaternary ammonium and a primary amine bound to the phosphate group, respectively.[147] Surface plasmon resonance[148] and resonance energy transfer[149] studies have shown that cyt *c* presents no significant electrostatic affinity for such lipids. Recent surface-enhanced resonance Raman (SERR) and RR investigations, on the other hand, demonstrated high-affinity binding of cyt *c* to model systems containing amino and ammonium functional groups[150,151] and to PE/PC-containing liposomes,[144] which is specifically mediated by inorganic and organic phosphate anions at millimolar levels.[150,151] Interestingly, under these conditions, the adsorbed protein reacts efficiently with H_2O_2 at submillimolar concentrations.[144] The reaction does not lead to the bleaching (destruction of the porphyrin chromophore) of the heme group but is restricted to sulfur oxidation of the axial ligand Met80, thus leading to its detachment from the heme iron, to form a OH^-/His coordinated species. This ligand exchange leads to an increase in the peroxidase activity by 1 order of magnitude, accompanied by an even higher increment in the electrocatalytic activity toward hydrogen peroxide, comparable to an iso-cyt *c* variant holding similar axial coordination.[49] The oxidation of Met80 results in a 125 mV downshift of the reduction potential,[144] hence implying the loss of its electron shuttling ability. The fraction of oxidized protein exhibits a strong linear dependence with pH that is consistent with the uptake of one proton per incoming electron, similar to bona fide peroxidases.[152,153]

These findings suggest a possible additional pathway for membrane permeabilization.[144] Specifically, the rise of hydrogen peroxide concentration to submillimolar levels that characterizes the initiation of apoptosis[154] appears to be sufficient to chemically modify a fraction of the cyt *c* molecules that interact (via phosphate anions) with the PE and PC membrane components. The modified protein is a stable peroxidase that could later bind CL and catalyze its oxidation, thus facilitating the liberation of pro-apoptotic factors, including unmodified cyt *c*.

Tuning Heme Midpoint Potential and Heme Axial Ligation To Swap Electron Transfer and Peroxidase Activity. The alternative axial coordinations of cyt *c* are all characterized by significant downshifts of the reduction potentials compared to that of the native protein and, therefore, are not capable of exerting efficient electron shuttling in the respiratory chain. This loss of function is paralleled by the gain of peroxidatic, pseudoperoxidatic, and myoglobin-like activity (Table 2). While native cyt *c* behaves as a weak peroxidase,[155] Met80 detachment leads to a significant increment of activity that is often ascribed to the presence of small amounts of pentacoordinated high-spin species[22] with distinct magnetic properties,[106] a drastically lowered reduction potential, and high solvent accessibility to the heme iron.[156]

Notably, high activities have also been attained in the absence of detectable high-spin species. This is, for example, the case of the cyt *c* nitrated at Tyr74, which exhibits an early alkaline transition.[30] Parallel acid−base RR titrations and peroxidatic activity determinations of this variant showed excellent correlations between the measured enzymatic activity and the concentration of the alkaline conformer.[157] Furthermore, titrations with CL of the different cyt *c* variants described in the previous sections also showed increasing overall peroxidatic activities that can be quantitatively correlated with the relative concentrations of the different alternative conformations determined by RR and their intrinsic enzymatic activities.[23] Nonetheless, these findings do not imply that the enzymatically active species are indeed the alternative six-coordinated low-spin forms, but most likely, they suggest that these alternative forms are prone to undergoing the required subsequent conformational changes in the presence of the electron donor and hydrogen peroxide. Although it is clear that low-spin to high-spin transitions of different heme proteins result in significant increments of the peroxidase activities,[158] it has also been argued that weakening (without breakage) of the Met80/Fe bond is sufficient to induce activity.[94]

Cyt *c* as an Electron Shuttle in a Complex Electrostatic Environment. Cyt *c* shuttles electrons from complex III to complex IV in a highly anisotropic environment. At the inner mitochondrial membrane, protons are pumped across the membrane to generate an electrochemical gradient, adding to the effects of the surface and dipole potentials to yield a strong interfacial electric field.[159] At biological membranes, the local interfacial electric fields arise from contributions of (i) the transmembrane potential, which is generated by the differences in anion and cation concentrations of the two bulk phases separated by the membrane; (ii) the surface potential, due to the interaction of the charged headgroups and solution electrolytes at the interface; and (iii) the dipole potential that originated in the alignment of the dipolar residues of the membrane and the interfacial water molecules.[159] Altogether, these contributions result in an interfacial electric field of 10^8−10^9 V m^{-1}.

DOI: 10.1021/acs.biochem.5b01385
Biochemistry 2016, 55, 407−428

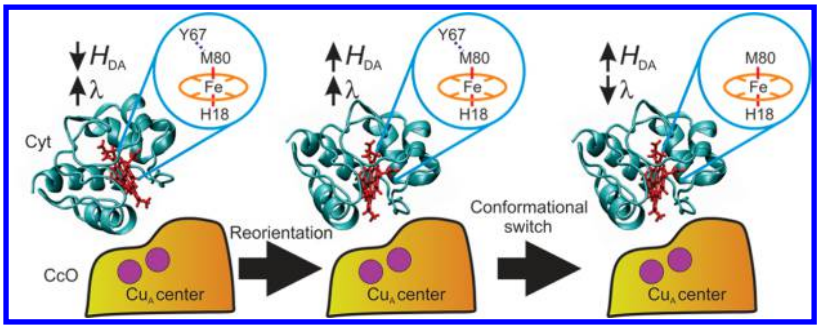

Figure 11. Schematic representation of the gated electron transfer mechanism. Cytochrome *c* forms an initial electrostatic complex with cyt *c* oxidase that is not optimized in terms of donor−acceptor electronic coupling, H_{DA}, and reorganization energy, λ. Before electron transfer can proceed, cyt *c* needs to reorient to achieve a sufficiently high H_{AD}. The new orientation favors the disruption of the Tyr67−Met80 H-bond, thus lowering λ and providing a complex optimized for efficient electron transfer. Both steps, reorientation and conformational switching, are strongly modulated by the interfacial electric field.

The artificial metal electrode−self-assembled monolayer (SAM)−solution interfaces reproduce some essential characteristics of the biological solution−lipid bilayer−solution interfaces, including the presence and magnitude of strong local electric fields. In the metal electrode, they originate in the potential drop across the SAM, and its magnitude is determined by the potential of zero charge of the metal, the applied potential, the tail group and chain length of the SAMs, and the electrolyte composition. This high field as well as electrostatic contacts with partner redox proteins and lipids may affect the structure and dynamics of cyt *c* in a way that is not necessarily deleterious for the different functions. On the contrary, the interfacial field may favor alternative conformations that optimize electron transfer kinetics or, eventually, induce alternative conformations with new functions.

Long-range protein electron transfer reactions can be rationalized in terms of Marcus' theory (equation below), which states that the ET rate constant (k_{ET}) is determined, among other factors, by the reorganization energy λ and the donor/acceptor (D/A) electronic coupling H_{DA}.[160,161] The reorganization energy is closely related to the free energy of activation, $\Delta G^{\ddagger}$, and represents the (hypothetical) change in free energy if the reactant state were to distort to the equilibrium nuclear configuration of the product state without actual transfer of the electron. Meanwhile, H_{DA} can be rationalized in terms of the overlap of the molecular orbitals of the donor and acceptor, which in the case of protein ET is mediated by the protein matrix and water molecules acting as a "molecular wire" between both redox centers. As a rule of thumb, high H_{DA} values and low λ values result in a high k_{ET}

$$k_{ET} = \frac{2\pi}{\hbar} |H_{DA}|^2 \frac{1}{\sqrt{4\pi\lambda k_B T}} \exp\left[-\frac{(\Delta G + \lambda)^2}{4\lambda k_B T}\right]$$

Before the electron transfer reaction proceeds, cyt *c* establishes transient redox complexes with its natural redox partners, which are stabilized mainly by electrostatic interactions. The following sections discuss how these contacts and the interfacial electric field may modulate the kinetic parameters, in particular H_{DA} and λ. The studies described employ a biomimetic setup consisting of nanostructured electrodes coated with self-assembled monolayers of carboxyl- or phosphate-terminated alkanethiols. This allows reproduction of essential features of protein−protein and protein−lipid interactions under simultaneous electrochemical and spectroscopic control of the adsorbed protein by means of time-resolved surface-enhanced RR spectroelectrochemistry.[162−165] This methodology provides simultaneous information about cyt *c* reorientation, axial coordination, electron exchange, and spin state along the redox reaction over a broad time window. Furthermore, the setup allows for fine-tuning of the interfacial electric field by manipulation of (i) the solution pH, (ii) the electrode potential, (iii) the thickness and composition of the biomimetic film, and (iv) the ionic strength.

Low Electric Fields: Alternative Complex Conformations. At physiological pH, cyt *c* presents net positive charge determined by a ring of protonated lysine residues surrounding the partially exposed heme edge. This positive patch establishes electrostatic contacts with negative counterparts in natural and biomimetic complexes, thus determining the coarse protein orientation. In addition, the large dipole moment, ~340 D,[166] interacts with the local fields influencing the orientation and rotational dynamics of the protein. A combination of theoretical and experimental results shows that there is no complex conformation that concurrently yields both an optimal binding free energy and maximal H_{DA}.[167−169] The average H_{DA} value depends not only on the coarse protein orientation but also on the disposition of the side chains and water molecules that mediate complex formation. In turn, the average protein orientation results from the interplay between the specific electrostatic contacts and the interaction between the interfacial field with the protein dipole moment. Moderate fields result in suboptimal H_{DA} values and hinder protein dynamics. The electron transfer reaction is then governed by the rate of the reorientation process that allows cyt *c* to achieve orientations that result in high H_{DA} values. Therefore, in this regime, the redox reaction is a gated process (Figure 11). On the other hand, at very low electric fields, protein reorientation is fast and thus conformational sampling and electron tunneling are uncoupled.[164,167−169]

This hypothesis was experimentally corroborated by designing a surface mutant, Lys87Cys, which according to theoretical predictions abolishes contacts that stabilize low electronic coupling orientations.[170] Further verification of the gated electron transfer mechanism arises from the negative kinetic impact of hindering protein dynamics, either through covalent immobilization of cyt *c* or by increasing solvent viscosity.[169] Altogether, these studies demonstrated that the electronic coupling of cyt *c* is strongly modulated by large and small amplitude dynamics of the protein and interfacial water molecules in the electrostatic complexes. Both types of fluctuations are influenced by local electric fields of biologically

DOI: 10.1021/acs.biochem.5b01385
Biochemistry 2016, 55, 407−428

relevant magnitude and contribute to the modulation of the electron transfer kinetics.

Moderately High Electric Fields: Alternative Second-Sphere Conformations. There has been some debate about whether residues Met80 and Tyr67 are hydrogen-bonded,[14,30,138,171−173] as this interaction would render Tyr67 a second-sphere ligand of the heme Fe that could participate in fine-tuning of the electronic properties. Analysis of the Tyr67−Met80 interaction using molecular dynamics simulations and a search algorithm that implements specific parameters for S atom acceptors[174] shows that, although through a relatively weak and fluctuating interaction, Tyr67 and Met80 can be regarded as H-bonded.[139] Indeed, Tyr67 has been proposed to be crucial in controlling cyt *c* structure and function through an extended H-bonding network.[137] To assess the importance of the H-bond interaction, the Tyr67Phe variant was studied.[139] Computational and experimental results showed that disruption of the Tyr67−Met80 bond trough mutation affects the protein's secondary structure. Strikingly, these minor structural variations are similar to those observed for the wild-type protein in biomimetic electrostatic complexes and involve Ω loops 20−30 and 70−85, respectively. Thus, as sufficiently high electric fields, the Tyr67−Met80 bond may act as a relay between the protein matrix and the redox center.[139] Indeed, under the influence of low interfacial electric fields, the electron transfer reorganization energy of cyt *c* is ∼0.6 eV. This value drops by a factor of 2 upon disruption of the Tyr67−Met80 bond, by either application of moderately high electric fields or the Tyr67Phe mutation, thus indicating that the Tyr67−Met80 H-bond is a key element of the conformational switch between high- and low-λ forms of native cyt *c*. The transition arises from the collective perturbation of the dynamics and average position of the amino acid residues and nearby water structural molecules, and this dynamical change can be achieved through the disruption of the Tyr67−Met80 bond.[139]

The conformational change between the high- and low-λ forms is activated by deformations of the flexible Ω loops that contain most of the lysine residues that constitute the protein binding site for biomimetic systems and natural redox partners,[167,168,175−177] thus suggesting that a similar mechanism of electron transfer optimization may be triggered upon interactions of cyt *c* with complexes III and IV (Figure 11).

High Electric Fields: Alternative First-Sphere Conformations. The axial coordination of the cyt *c* state is susceptible to the presence of homogeneous electric fields and to the formation of specific electrostatic contacts. Recent experimental studies allow for disentanglement of both contributions to the apparition of the alternative first-sphere coordinations, as the biomimetic model systems can be tailored to yield fields of varying magnitudes without affecting contact formation.

Increasing the interfacial electric field elicits detachment of Met80, leading to a coordination equilibrium between different substrates, in which the sixth coordination site of the heme remains vacant, leading to a five-coordinated high-spin configuration, or is occupied by different alternative ligands, including a water molecule, hydroxyl, lysine, or histidine, depending on the specific conditions.[178] At high electric fields, the alternative forms of cyt *c* can account for more than 75% of total adsorbed protein.[163,165] This effect has been attained not only on biomimetic electrodes but also on other model systems such as polyelectrolytes,[179] phospholipid vesicles,[117,180] and even the electrostatic complex with cyt *c* oxidase.[181] Theoretical studies show that the applied electric field exerts no appreciable effect on the strength of the Met80−Fe bond.[182] Instead, the interaction between the field and the dipole moments of the different segments of the α-helices elicits structural rearrangements that yield the alternative first-sphere conformations.[156]

The effect of the specific interaction between cyt *c* and cardiolipin differs from that of homogeneous electric fields. In this case, establishment of specific contacts exerts similar effects on all cyt *c* molecules as they all converge to a common bis-His form (see above).[23] Notably, all alternative axial conformations present very negative redox potentials that render cyt *c* unsuitable for participating in the electron transport, but they exhibit enhanced peroxidatic activities.

In summary, the strength of the electric field produces varying effects on the conformation of cyt *c*. Low fields act on the complex formation affecting protein (re)orientation, thus modulating H_{DA}. The field may also affect the protein structure at the level of the second-sphere ligand Tyr67, thus lowering the reorganization energy, while even higher fields affect first-sphere ligands.

Antibody Probes of Altered Cyt *c* Conformation. By the late 1960s, it had already been established that antibody recognition of globular proteins, i.e., those with hydrophobic interiors and hydrophilic exteriors, is sensitive to the conformation of those antigens.[183] There was a flurry of activity in the mid to late 1980s attempting to use peptides to mimic epitopes on globular proteins for application in vaccine development. Although this was at odds with the established concept that antibody recognition of globular proteins is conformationally restricted, initially there appeared to be encouraging data in support of this effort. However, an artifact in the assays employed that had not been previously appreciated was shown to be responsible for false positive results; i.e., antibodies reactive with non-native forms of the protein antigens had been confused for antibodies to the native forms in assays in which antigens were adsorbed to a solid support.[184,185] For example, conformational variants of cyt *c* arise when coupling the protein to a carrier and/or emulsifying cyt *c* in mineral oil to enhance immunogenicity, and these forms elicit antibodies that cannot be distinguished from antibodies to native cyt *c* in direct solid phase immunoassays because some antigen molecules are denatured when adsorbed to a solid support.

Distinction between monoclonal antibodies (mAbs) specific for native versus non-native forms of an antigen can be obtained by testing the ability of the native protein antigen in solution to inhibit binding of the antibody to the antigen in the solid phase.[184,185] Employing this approach, it is possible to identify antibodies reactive with both native and non-native forms of a protein antigen that may have different applications in research. For example, a mAb specific for the native form may be useful for immunofluorescence studies to determine expression and location of an antigen *in situ* and for immunoprecipitation as, for example, to isolate binding partners, whereas a mAb specific for a non-native form may be useful for Western blotting where the protein is usually denatured prior to electrophoresis.

In addition to numerous mAbs shown to bind native cyt *c*, several mAbs that bound cyt *c* adsorbed to immunoassay plates and could not be inhibited by the presence of native cyt *c* in the solution phase were, thus, determined to be reactive with non-native forms of cyt. One such antibody, mAb 7H8, shown to bind the carboxyl terminus of cyt *c* (residues 93−104), was

DOI: 10.1021/acs.biochem.5b01385
Biochemistry 2016, 55, 407−428

found to be useful for detection of cyt *c* in Western blots. This provided the proof, by comparison of cytosolic and mitochondrial extracts, that cyt translocates to the cytosol in apoptotic cells.[186] None of several mAbs specific for the native conformation of cyt *c* were able to detect the antigen in Western blots. However, these mAbs did show redistribution of cyt *c* to the cytoplasm by immunofluorescence analysis.

Another mAb that bound a non-native form of cyt *c*, mAb 1D3, did not react with cyt *c* in Western blots but did label cyt *c* in cells very early in apoptosis at a stage when bona fide indicators of apoptosis are not yet apparent.[36] The particular conformation that mAb 1D3 recognizes also occurs when cyt *c* is bound to phospholipids. This suggests that mAb 1D3 may recognize cyt *c* bound to CL at a step leading to its translocation from the mitochondrial intermembrane space.[22] The conformation of cyt *c* in this context is not globally denatured because mAbs such as mAb 7H8 that bind well to short peptides did not label cyt *c* in apoptotic cells. Cytochrome *c* extracted from the apoptotic cells with detergent could not be immunoprecipitated with mAb 1D3, indicating that the altered cyt *c* conformation was dependent on detergent-sensitive binding of cyt *c* to some other component, possibly CL.[36]

On the basis of binding to cyts *c* from various species and comparison of their amino acid sequences, the region of the cyt *c* polypeptide chain recognized by mAb 1D3 was shown to involve residue Pro44 (Figure 1b). In addition, a peptide containing residues 40−54 was able to inhibit the binding of mAb 1D3 to cyt *c*-coated immunoassay plates, albeit at relatively high concentrations. Longer peptides, including cyanogen bromide-cleaved peptides 1−65 and 1−80, showed more effective inhibition with increasing peptide lengths, suggesting that the conformation of cyt *c* recognized by mAb 1D3 is nativelike but not actually native. Unlike mAb 1D3, a mAb specific for the region around residue 44 on native cyt *c* failed to bind even the long cyanogen bromide-cleaved peptides and was shown to involve discontinuous segments, including residues 26 and 27 as well as the segment around residue Pro44.[187] These two segments are H-bonded in native cyt *c* where the imidazole nitrogen of His26 is H-bonded to the carbonyl oxygen of residue Pro44. This H-bond is lost in the alkaline conformation of cyt *c*, a form that mAb 1D3 has also been shown to bind.[24,36] In Figure 2g, the 40−57 segment in the model of yeast iso-1-cyt *c* is displaced at alkaline pH, consistent with an altered epitope in this region of the polypeptide chain.

The altered conformation of cyt *c* recognized by mAb 1D3 arises in multiple contexts. In addition to resulting from the effects of bound phospholipids and alkaline pH, it has been shown to occur as a consequence of covalent modification by nitration at certain tyrosine residues and dislocation of the Met80−heme ligation due to amino acid substitution.[24] It seems likely that in these various contexts epitopes other than that recognized by mAb 1D3 become exposed. Indeed, distinct cellular locations have been observed in two of these contexts, suggesting exposure of unique determinants for cellular localization. Thus, CL-bound cyt is localized to mitochondria, whereas loss of the Met80−heme ligation due to amino acid substitution results in nuclear and cytoplasmic localization of cyt *c*.[22,24,36] While positive immunostaining with mAb 1D3 alone cannot define the insult leading to the conformational change in cyt *c*, in conjunction with the pattern of staining defining the cellular localization, mAb 1D3 immunostaining may provide insights into the context for the conformational change.

CONCLUSIONS AND PERSPECTIVES

A growing body of evidence indicates that the structural flexibility of cyt *c*, partly conferred by evolutionary conservation of Tyr67, permits switching between native and alternative conformations. Some biological functions of these alternative conformations have been elucidated, while others await further investigation. The biosynthesis and maturation of cyt *c* involve transient axial ligation of its heme by holo-cyt *c* synthetase, changes in oxidation state, and a perfectly funneled energy landscape during folding that jointly ensure adoption of the native conformation. Aside from electron transfer, mature cyt *c* responds to cellular stressors via changes in coordination, geometry, and redox properties of its heme center as well as conformational changes of the protein matrix to form alternative conformers. Some of these alternative conformers of cyt *c* have been shown to reside outside the mitochondrion, at least transiently.

One aspect that is open for investigation concerns the association of native and alternative conformations of cyt *c* with other protein partners in the cell. Not less enigmatic is the role of the peroxidase activity of cyt *c* in apoptosis and other pathways. Structural studies comparing yeast and mammalian cyts *c* suggest that both steric factors near the active site and the opening of the heme crevice itself are unique features that evolved in higher organisms to limit peroxidase activity and finely tune the onset of apoptosis.[49] The recent identification of drugs that could selectively inhibit the peroxidase activity of cyt *c* may help distinguish between its canonical and secondary functions.[188]

In general, ancestral proteins involved in apoptosis carry substantial intrinsic plasticity to meet the demands of different organisms and biological niches.[189] For example, the release of cyt *c* into the cytosol has been well-documented in both yeast and mammals; however, yeast iso-cyt *c* does not activate caspases.[190] In mammals, imbalances in nitric oxide homeostasis that are favorable for Tyr nitration would stimulate cyt *c* peroxidase activity whereas heme nitrosylation has the opposite effect.[35] Because native cyt *c* is essentially inert toward heme axial ligand substitution, a conformational change that weakens the coordination sphere of the heme must precede nitric oxide binding. CL has been shown to enhance the reactivity of cyt *c* toward NO, making it a plausible biological partner for the pro-apoptotic effects of nitrosylated cyt *c*.[191] It is currently unclear whether the pro-apoptotic effects of nitrosylated cyt *c* are triggered by alternative conformations anteceding heme nitrosylation, by heme nitrosylation per se, or by downstream conformational modifications that promote apoptosome assembly. The biogenesis of cyt *c* takes place in the cytosol and the mitochondrion, two compartments with distinct redox properties, which may have shaped its ability to sense the environment, swap functions, and develop self-reliant means for cellular transit. While the pool of free intracellular cyt *c* has been estimated to be approximately 10−15%,[192,193] it is notable that its alternative conformers translocate more readily across compartments, raising the possibility that these species may act at the forefront of cellular decisions. On the basis of its tunable peroxidase activity, sensitivity to electric fields, and translocation across cellular compartments, we posit that cyt *c* is well-suited to operate as a redox sensor. Overall, the data presented herein clearly support the idea that molecular

DOI: 10.1021/acs.biochem.5b01385
Biochemistry 2016, 55, 407−428

flexibility in cyt *c* maintained through evolution allows this heme protein to play a wide range of functions in addition to its well-defined respiratory and apoptotic activities. Fluctuations in the physicochemical properties of the cellular environment as well as modifications in the protein moiety can lead to conformational changes that ultimately affect the heme microenvironment. Structural biology and immunochemical studies are assisting in the characterization and identification, both *in vitro* and *in vivo*, of a collection of biologically relevant conformations of cyt *c*. Further research is needed to reveal the occurrence, timing, and implications of alternative conformations of cyt *c* in human physiology and pathophysiology, in particular in the context of processes associated with changes in mitochondrial and cellular redox homeostasis.

AUTHOR INFORMATION

Corresponding Author

*E-mail: rradi@fmed.edu.uy or rafael.radi@gmail.com.

Notes

The authors declare no competing financial interest.

ACKNOWLEDGMENTS

This work was supported by grants of Agencia Nacional de Investigación e Innovación (FCE_2014_104233), Universidad de la República (CSIC-UdelaR), and the National Institutes of Health (RO1 AI095173) to R.R., ANPCyT (PICT 2010-070 and 2011-1249) and UBACyT (Grant 20020130100206BA) to D.H.M., and intramural support from the Center for Pediatrics and Adolescent Medicine, Medical Center, University of Freiburg, to L.H. Additional support was obtained from Programa de Desarrollo de Ciencias Básicas (PEDECIBA), Centro de Biología Estructural del Mercosur (CeBEM), CONICET, and Ridaline and Biriden through Fundación Manuel Pérez.

ABBREVIATIONS

cyt *c*, cytochrome *c*; CL, cardiolipin; MIA40, mitochondrial intermembrane space assembly 40; Erv1, essential for respiration and vegetative growth 1; Apaf-1, apoptotic peptidase activating factor 1; ET, electron transfer; SAM, self-assembled monolayers; PDB, Protein Data Bank.

REFERENCES

(1) Margoliash, E. (1972) Functional evolution of cytochrome *c*. In *The Harvey Lectures*, Series 66, pp 177−247, Academic Press, London.
(2) Bushnell, G. W., Louie, G. V., and Brayer, G. D. (1990) High-resolution three-dimensional structure of horse heart cytochrome c. *J. Mol. Biol. 214*, 585−595.
(3) Zaidi, S., Hassan, M. I., Islam, A., and Ahmad, F. (2014) The role of key residues in structure, function, and stability of cytochrome-c. *Cell. Mol. Life Sci. 71*, 229−255.
(4) Schmidt, T. R., Wildman, D. E., Uddin, M., Opazo, J. C., Goodman, M., and Grossman, L. I. (2005) Rapid electrostatic evolution at the binding site for cytochrome c on cytochrome c oxidase in anthropoid primates. *Proc. Natl. Acad. Sci. U. S. A. 102*, 6379−6384.
(5) Bertini, I., Grassi, E., Luchinat, C., Quattrone, A., and Saccenti, E. (2006) Monomorphism of human cytochrome c. *Genomics 88*, 669−672.
(6) Fumo, G., Spitzer, J. S., and Fetrow, J. S. (1995) A method of directed random mutagenesis of the yeast chromosome shows that the iso-1-cytochrome c heme ligand His18 is essential. *Gene 164*, 33−39.
(7) Roder, H., Elove, G. A., and Englander, S. W. (1988) Structural characterization of folding intermediates in cytochrome c by H-exchange labelling and proton NMR. *Nature 335*, 700−704.
(8) Sosnick, T. R., Mayne, L., Hiller, R., and Englander, S. W. (1994) The barriers in protein folding. *Nat. Struct. Biol. 1*, 149−156.
(9) Wu, L. C., Laub, P. B., Elove, G. A., Carey, J., and Roder, H. (1993) A noncovalent peptide complex as a model for an early folding intermediate of cytochrome c. *Biochemistry 32*, 10271−10276.
(10) San Francisco, B., Bretsnyder, E. C., and Kranz, R. G. (2013) Human mitochondrial holocytochrome c synthase's heme binding, maturation determinants, and complex formation with cytochrome c. *Proc. Natl. Acad. Sci. U. S. A. 110*, E788−797.
(11) Kapralov, A. A., Yanamala, N., Tyurina, Y. Y., Castro, L., Samhan-Arias, A., Vladimirov, Y. A., Maeda, A., Weitz, A. A., Peterson, J., Mylnikov, D., Demicheli, V., Tortora, V., Klein-Seetharaman, J., Radi, R., and Kagan, V. E. (2011) Topography of tyrosine residues and their involvement in peroxidation of polyunsaturated cardiolipin in cytochrome c/cardiolipin peroxidase complexes. *Biochim. Biophys. Acta, Biomembr. 1808*, 2147−2155.
(12) Barker, P. D., and Ferguson, S. J. (1999) Still a puzzle: why is haem covalently attached in c-type cytochromes? *Structure 7*, R281−290.
(13) Heineman, W. R., Norris, B. J., and Goelz, J. F. (1975) Measurement of enzyme E'values by optically transparent thin layer electrochemical cells. *Anal. Chem. 47*, 79−84.
(14) Luntz, T. L., Schejter, A., Garber, E. A., and Margoliash, E. (1989) Structural significance of an internal water molecule studied by site-directed mutagenesis of tyrosine-67 in rat cytochrome c. *Proc. Natl. Acad. Sci. U. S. A. 86*, 3524−3528.
(15) Kawai, C., Prado, F. M., Nunes, G. L., Di Mascio, P., Carmona-Ribeiro, A. M., and Nantes, I. L. (2005) pH-Dependent interaction of cytochrome c with mitochondrial mimetic membranes: the role of an array of positively charged amino acids. *J. Biol. Chem. 280*, 34709−34717.
(16) Koppenol, W. H., and Margoliash, E. (1982) The asymmetric distribution of charges on the surface of horse cytochrome c. Functional implications. *J. Biol. Chem. 257*, 4426−4437.
(17) Huttemann, M., Pecina, P., Rainbolt, M., Sanderson, T. H., Kagan, V. E., Samavati, L., Doan, J. W., and Lee, I. (2011) The multiple functions of cytochrome c and their regulation in life and death decisions of the mammalian cell: From respiration to apoptosis. *Mitochondrion 11*, 369−381.
(18) Mordas, A., and Tokatlidis, K. (2015) The MIA Pathway: A Key Regulator of Mitochondrial Oxidative Protein Folding and Biogenesis. *Acc. Chem. Res. 48*, 2191−2199.
(19) Greenwood, C., and Palmer, G. (1965) Evidence for the existence of two functionally distinct forms cytochrome c manomer at alkaline pH. *J. Biol. Chem. 240*, 3660−3663.
(20) Wilson, M. T., and Greenwood, C. (1996) The alkaline transition in ferrycytochrome c. In *Cytochrome C: A Multidisciplinary Approach* (Scott, R. A., and Mauk, A. G., Eds.) pp 611−634, University Science Books, Sausalito, CA.
(21) Theorell, H., and Åkesson, A. (1941) Studies on cytochrome c. II. The optical properties of pure cytochrome c and some of its derivatives. *J. Am. Chem. Soc. 63*, 1812−1818.
(22) Kagan, V. E., Tyurin, V. A., Jiang, J., Tyurina, Y. Y., Ritov, V. B., Amoscato, A. A., Osipov, A. N., Belikova, N. A., Kapralov, A. A., Kini, V., Vlasova, II, Zhao, Q., Zou, M., Di, P., Svistunenko, D. A., Kurnikov, I. V., and Borisenko, G. G. (2005) Cytochrome c acts as a cardiolipin oxygenase required for release of proapoptotic factors. *Nat. Chem. Biol. 1*, 223−232.
(23) Capdevila, D. A., Oviedo Rouco, S., Tomasina, F., Tortora, V., Demicheli, V., Radi, R., and Murgida, D. H. (2015) Active Site Structure and Peroxidase Activity of Oxidatively Modified Cytochrome c Species in Complexes with Cardiolipin. *Biochemistry 54*, 7491−7504.
(24) Godoy, L. C., Munoz-Pinedo, C., Castro, L., Cardaci, S., Schonhoff, C. M., King, M., Tortora, V., Marin, M., Miao, Q., Jiang, J. F., Kapralov, A., Jemmerson, R., Silkstone, G. G., Patel, J. N., Evans, J. E., Wilson, M. T., Green, D. R., Kagan, V. E., Radi, R., and Mannick, J.

DOI: 10.1021/acs.biochem.5b01385
Biochemistry 2016, 55, 407−428

B. (2009) Disruption of the M80-Fe ligation stimulates the translocation of cytochrome c to the cytoplasm and nucleus in nonapoptotic cells. *Proc. Natl. Acad. Sci. U. S. A. 106*, 2653−2658.
(25) Tuominen, E. K., Wallace, C. J., and Kinnunen, P. K. (2002) Phospholipid-cytochrome c interaction: evidence for the extended lipid anchorage. *J. Biol. Chem. 277*, 8822−8826.
(26) Santucci, R., Sinibaldi, F., Patriarca, A., Santucci, D., and Fiorucci, L. (2010) Misfolded proteins and neurodegeneration: role of non-native cytochrome c in cell death. *Expert Rev. Proteomics 7*, 507−517.
(27) Hoye, A. T., Davoren, J. E., Wipf, P., Fink, M. P., and Kagan, V. E. (2008) Targeting mitochondria. *Acc. Chem. Res. 41*, 87−97.
(28) Josephs, T. M., Liptak, M. D., Hughes, G., Lo, A., Smith, R. M., Wilbanks, S. M., Bren, K. L., and Ledgerwood, E. C. (2013) Conformational change and human cytochrome c function: mutation of residue 41 modulates caspase activation and destabilizes Met-80 coordination. *JBIC, J. Biol. Inorg. Chem. 18*, 289−297.
(29) Cassina, A. M., Hodara, R., Souza, J. M., Thomson, L., Castro, L., Ischiropoulos, H., Freeman, B. A., and Radi, R. (2000) Cytochrome c nitration by peroxynitrite. *J. Biol. Chem. 275*, 21409−21415.
(30) Abriata, L. A., Cassina, A., Tortora, V., Marin, M., Souza, J. M., Castro, L., Vila, A. J., and Radi, R. (2009) Nitration of solvent-exposed tyrosine 74 on cytochrome c triggers heme iron-methionine 80 bond disruption. Nuclear magnetic resonance and optical spectroscopy studies. *J. Biol. Chem. 284*, 17−26.
(31) Josephs, T. M., Morison, I. M., Day, C. L., Wilbanks, S. M., and Ledgerwood, E. C. (2014) Enhancing the peroxidase activity of cytochrome c by mutation of residue 41: implications for the peroxidase mechanism and cytochrome c release. *Biochem. J. 458*, 259−265.
(32) De Rocco, D., Cerqua, C., Goffrini, P., Russo, G., Pastore, A., Meloni, F., Nicchia, E., Moraes, C. T., Pecci, A., Salviati, L., and Savoia, A. (2014) Mutations of cytochrome c identified in patients with thrombocytopenia THC4 affect both apoptosis and cellular bioenergetics. *Biochim. Biophys. Acta, Mol. Basis Dis. 1842*, 269−274.
(33) Lett, C. M., and Guillemette, J. G. (2002) Increasing the redox potential of isoform 1 of yeast cytochrome c through the modification of select haem interactions. *Biochem. J. 362*, 281−287.
(34) Ascenzi, P., Coletta, M., Wilson, M. T., Fiorucci, L., Marino, M., Polticelli, F., Sinibaldi, F., and Santucci, R. (2015) Cardiolipin-cytochrome c complex: Switching cytochrome c from an electron-transfer shuttle to a myoglobin- and a peroxidase-like heme-protein. *IUBMB Life 67*, 98−109.
(35) Schonhoff, C. M., Gaston, B., and Mannick, J. B. (2003) Nitrosylation of cytochrome c during apoptosis. *J. Biol. Chem. 278*, 18265−18270.
(36) Jemmerson, R., Liu, J., Hausauer, D., Lam, K. P., Mondino, A., and Nelson, R. D. (1999) A conformational change in cytochrome c of apoptotic and necrotic cells is detected by monoclonal antibody binding and mimicked by association of the native antigen with synthetic phospholipid vesicles. *Biochemistry 38*, 3599−3609.
(37) Yu, X., Acehan, D., Menetret, J. F., Booth, C. R., Ludtke, S. J., Riedl, S. J., Shi, Y., Wang, X., and Akey, C. W. (2005) A structure of the human apoptosome at 12.8 A resolution provides insights into this cell death platform. *Structure 13*, 1725−1735.
(38) Zhou, M., Li, Y., Hu, Q., Bai, X. C., Huang, W., Yan, C., Scheres, S. H., and Shi, Y. (2015) Atomic structure of the apoptosome: mechanism of cytochrome c- and dATP-mediated activation of Apaf-1. *Genes Dev. 29*, 2349−2361.
(39) Boehning, D., Patterson, R. L., Sedaghat, L., Glebova, N. O., Kurosaki, T., and Snyder, S. H. (2003) Cytochrome c binds to inositol (1,4,5) trisphosphate receptors, amplifying calcium-dependent apoptosis. *Nat. Cell Biol. 5*, 1051−1061.
(40) Bruey, J. M., Ducasse, C., Bonniaud, P., Ravagnan, L., Susin, S. A., Diaz-Latoud, C., Gurbuxani, S., Arrigo, A. P., Kroemer, G., Solary, E., and Garrido, C. (2000) Hsp27 negatively regulates cell death by interacting with cytochrome c. *Nat. Cell Biol. 2*, 645−652.
(41) Codina, R., Vanasse, A., Kelekar, A., Vezys, V., and Jemmerson, R. (2010) Cytochrome c-induced lymphocyte death from the outside in: inhibition by serum leucine-rich alpha-2-glycoprotein-1. *Apoptosis 15*, 139−152.
(42) Feng, Y., Roder, H., Englander, S. W., Wand, A. J., and Di Stefano, D. L. (1989) Proton resonance assignments of horse ferricytochrome c. *Biochemistry 28*, 195−203.
(43) Feng, Y., and Englander, S. W. (1990) Salt-dependent structure change and ion binding in cytochrome c studied by two-dimensional proton NMR. *Biochemistry 29*, 3505−3509.
(44) Feng, Y., Roder, H., and Englander, S. W. (1990) Redox-dependent structure change and hyperfine nuclear magnetic resonance shifts in cytochrome c. *Biochemistry 29*, 3494−3504.
(45) Feng, Y. Q., Roder, H., and Englander, S. W. (1990) Assignment of paramagnetically shifted resonances in the 1H NMR spectrum of horse ferricytochrome c. *Biophys. J. 57*, 15−22.
(46) Leszczynski, J. F., and Rose, G. D. (1986) Loops in globular proteins: a novel category of secondary structure. *Science 234*, 849−855.
(47) Louie, G. V., and Brayer, G. D. (1990) High-resolution refinement of yeast iso-1-cytochrome c and comparisons with other eukaryotic cytochromes c. *J. Mol. Biol. 214*, 527−555.
(48) Liptak, M. D., Fagerlund, R. D., Ledgerwood, E. C., Wilbanks, S. M., and Bren, K. L. (2011) The proapoptotic G41S mutation to human cytochrome c alters the heme electronic structure and increases the electron self-exchange rate. *J. Am. Chem. Soc. 133*, 1153−1155.
(49) McClelland, L. J., Mou, T. C., Jeakins-Cooley, M. E., Sprang, S. R., and Bowler, B. E. (2014) Structure of a mitochondrial cytochrome c conformer competent for peroxidase activity. *Proc. Natl. Acad. Sci. U. S. A. 111*, 6648−6653.
(50) Poulos, T. L., and Kraut, J. (1980) A hypothetical model of the cytochrome c peroxidase. cytochrome c electron transfer complex. *J. Biol. Chem. 255*, 10322−10330.
(51) Poulos, T. L., and Finzel, B. C. (1984) Heme enzyme structure and function. *Pept. Prot. Rev. 4*, 115−171.
(52) Gu, J., Yang, S., Rajic, A. J., Kurnikov, I. V., Prytkova, T. R., and Pletneva, E. V. (2014) Control of cytochrome c redox reactivity through off-pathway modifications in the protein hydrogen-bonding network. *Chem. Commun. (Cambridge, U. K.) 50*, 5355−5357.
(53) Bowman, S. E., and Bren, K. L. (2008) The chemistry and biochemistry of heme c: functional bases for covalent attachment. *Nat. Prod. Rep. 25*, 1118−1130.
(54) Haldar, S., Mitra, S., and Chattopadhyay, K. (2010) Role of protein stabilizers on the conformation of the unfolded state of cytochrome c and its early folding kinetics: investigation at single molecular resolution. *J. Biol. Chem. 285*, 25314−25323.
(55) Paul, S. S., Sil, P., Haldar, S., Mitra, S., and Chattopadhyay, K. (2015) Subtle Change in the Charge Distribution of Surface Residues May Affect the Secondary Functions of Cytochrome c. *J. Biol. Chem. 290*, 14476−14490.
(56) Weinkam, P., Pletneva, E. V., Gray, H. B., Winkler, J. R., and Wolynes, P. G. (2009) Electrostatic effects on funneled landscapes and structural diversity in denatured protein ensembles. *Proc. Natl. Acad. Sci. U. S. A. 106*, 1796−1801.
(57) Weinkam, P., Zimmermann, J., Romesberg, F. E., and Wolynes, P. G. (2010) The folding energy landscape and free energy excitations of cytochrome c. *Acc. Chem. Res. 43*, 652−660.
(58) Bryngelson, J. D., Onuchic, J. N., Socci, N. D., and Wolynes, P. G. (1995) Funnels, pathways, and the energy landscape of protein folding: a synthesis. *Proteins: Struct., Funct., Genet. 21*, 167−195.
(59) Maity, H., Rumbley, J. N., and Englander, S. W. (2006) Functional role of a protein foldon–an Omega-loop foldon controls the alkaline transition in ferricytochrome c. *Proteins: Struct., Funct., Genet. 63*, 349−355.
(60) Perroud, T. D., Bokoch, M. P., and Zare, R. N. (2005) Cytochrome c conformations resolved by the photon counting histogram: watching the alkaline transition with single-molecule sensitivity. *Proc. Natl. Acad. Sci. U. S. A. 102*, 17570−17575.
(61) Hong, X. L., and Dixon, D. W. (1989) NMR study of the alkaline isomerization of ferricytochrome c. *FEBS Lett. 246*, 105−108.

DOI: 10.1021/acs.biochem.5b01385
Biochemistry 2016, 55, 407−428

(62) Ferrer, J. C., Guillemette, J. G., Bogumil, R., Inglis, S. C., Smith, M., and Mauk, A. G. (1993) Identification of Lys79 as an iron ligand in one form of alkaline yeast iso-1-ferricytochrome c. *J. Am. Chem. Soc. 115*, 7507−7508.
(63) Bai, Y., Sosnick, T. R., Mayne, L., and Englander, S. W. (1995) Protein folding intermediates: native-state hydrogen exchange. *Science 269*, 192−197.
(64) Krishna, M. M., Maity, H., Rumbley, J. N., and Englander, S. W. (2007) Branching in the sequential folding pathway of cytochrome c. *Protein Sci. 16*, 1946−1956.
(65) Maity, H., Maity, M., and Englander, S. W. (2004) How cytochrome c folds, and why: submolecular foldon units and their stepwise sequential stabilization. *J. Mol. Biol. 343*, 223−233.
(66) Maity, H., Maity, M., Krishna, M. M., Mayne, L., and Englander, S. W. (2005) Protein folding: the stepwise assembly of foldon units. *Proc. Natl. Acad. Sci. U. S. A. 102*, 4741−4746.
(67) Panchenko, A. R., Luthey-Schulten, Z., and Wolynes, P. G. (1996) Foldons, protein structural modules, and exons. *Proc. Natl. Acad. Sci. U. S. A. 93*, 2008−2013.
(68) Krishna, M. M., Lin, Y., Mayne, L., and Englander, S. W. (2003) Intimate view of a kinetic protein folding intermediate: residue-resolved structure, interactions, stability, folding and unfolding rates, homogeneity. *J. Mol. Biol. 334*, 501−513.
(69) Fazelinia, H., Xu, M., Cheng, H., and Roder, H. (2014) Ultrafast hydrogen exchange reveals specific structural events during the initial stages of folding of cytochrome c. *J. Am. Chem. Soc. 136*, 733−740.
(70) Ziv, G., Thirumalai, D., and Haran, G. (2009) Collapse transition in proteins. *Phys. Chem. Chem. Phys. 11*, 83−93.
(71) Klein-Seetharaman, J., Oikawa, M., Grimshaw, S. B., Wirmer, J., Duchardt, E., Ueda, T., Imoto, T., Smith, L. J., Dobson, C. M., and Schwalbe, H. (2002) Long-range interactions within a nonnative protein. *Science 295*, 1719−1722.
(72) Lapidus, L. J., Yao, S., McGarrity, K. S., Hertzog, D. E., Tubman, E., and Bakajin, O. (2007) Protein hydrophobic collapse and early folding steps observed in a microfluidic mixer. *Biophys. J. 93*, 218−224.
(73) Russell, B. S., Melenkivitz, R., and Bren, K. L. (2000) NMR investigation of ferricytochrome c unfolding: detection of an equilibrium unfolding intermediate and residual structure in the denatured state. *Proc. Natl. Acad. Sci. U. S. A. 97*, 8312−8317.
(74) Colon, W., Wakem, L. P., Sherman, F., and Roder, H. (1997) Identification of the predominant non-native histidine ligand in unfolded cytochrome c. *Biochemistry 36*, 12535−12541.
(75) Elove, G. A., Bhuyan, A. K., and Roder, H. (1994) Kinetic mechanism of cytochrome c folding: involvement of the heme and its ligands. *Biochemistry 33*, 6925−6935.
(76) Takahashi, S., Yeh, S. R., Das, T. K., Chan, C. K., Gottfried, D. S., and Rousseau, D. L. (1997) Folding of cytochrome c initiated by submillisecond mixing. *Nat. Struct. Biol. 4*, 44−50.
(77) Tezcan, F. A., Winkler, J. R., and Gray, H. B. (1999) Probing Protein Folding with Substitution-Inert Metal Ions. Folding Kinetics of Co(III)-cytochrome c. *J. Am. Chem. Soc. 121*, 11918−11919.
(78) Gadsby, P. M., Peterson, J., Foote, N., Greenwood, C., and Thomson, A. J. (1987) Identification of the ligand-exchange process in the alkaline transition of horse heart cytochrome c. *Biochem. J. 246*, 43−54.
(79) Brandt, K. G., Parks, P. C., Czerlinski, G. H., and Hess, G. P. (1966) On the elucidation of the pH dependence of the oxidation-reduction potential of cytochrome c at alkaline pH. *J. Biol. Chem. 241*, 4180−4185.
(80) Hoang, L., Maity, H., Krishna, M. M., Lin, Y., and Englander, S. W. (2003) Folding units govern the cytochrome c alkaline transition. *J. Mol. Biol. 331*, 37−43.
(81) Assfalg, M., Bertini, I., Dolfi, A., Turano, P., Mauk, A. G., Rosell, F. I., and Gray, H. B. (2003) Structural model for an alkaline form of ferricytochrome C. *J. Am. Chem. Soc. 125*, 2913−2922.
(82) Döpner, S., Hildebrandt, P., Rosell, F. I., and Mauk, A. G. (1998) Alkaline Conformational Transitions of Ferricytochrome c Studied by Resonance Raman Spectroscopy. *J. Am. Chem. Soc. 120*, 11246−11255.
(83) Bradley, J. M., Silkstone, G., Wilson, M. T., Cheesman, M. R., and Butt, J. N. (2011) Probing a complex of cytochrome c and cardiolipin by magnetic circular dichroism spectroscopy: implications for the initial events in apoptosis. *J. Am. Chem. Soc. 133*, 19676−19679.
(84) Amacher, J. F., Zhong, F., Lisi, G. P., Zhu, M. Q., Alden, S. L., Hoke, K. R., Madden, D. R., and Pletneva, E. V. (2015) A Compact Structure of Cytochrome c Trapped in a Lysine-Ligated State: Loop Refolding and Functional Implications of a Conformational Switch. *J. Am. Chem. Soc. 137*, 8435−8449.
(85) McClelland, L. J., Seagraves, S. M., Khan, M. K., Cherney, M. M., Bandi, S., Culbertson, J. E., and Bowler, B. E. (2015) The response of Omega-loop D dynamics to truncation of trimethyllysine 72 of yeast iso-1-cytochrome c depends on the nature of loop deformation. *JBIC, J. Biol. Inorg. Chem. 20*, 805−819.
(86) Bandi, S., and Bowler, B. E. (2015) Effect of an Ala81His Mutation on the Met80 Loop Dynamics of Iso-1-cytochrome c. *Biochemistry 54*, 1729.
(87) Kinnunen, P. K., Koiv, A., Lehtonen, J. Y., Rytomaa, M., and Mustonen, P. (1994) Lipid dynamics and peripheral interactions of proteins with membrane surfaces. *Chem. Phys. Lipids 73*, 181−207.
(88) Kawai, C., Pessoto, F. S., Rodrigues, T., Mugnol, K. C., Tortora, V., Castro, L., Milicchio, V. A., Tersariol, I. L., Di Mascio, P., Radi, R., Carmona-Ribeiro, A. M., and Nantes, I. L. (2009) pH-sensitive binding of cytochrome c to the inner mitochondrial membrane. Implications for the participation of the protein in cell respiration and apoptosis. *Biochemistry 48*, 8335−8342.
(89) Rytomaa, M., Mustonen, P., and Kinnunen, P. K. (1992) Reversible, nonionic, and pH-dependent association of cytochrome c with cardiolipin-phosphatidylcholine liposomes. *J. Biol. Chem. 267*, 22243−22248.
(90) Rytomaa, M., and Kinnunen, P. K. (1994) Evidence for two distinct acidic phospholipid-binding sites in cytochrome c. *J. Biol. Chem. 269*, 1770−1774.
(91) Rytomaa, M., and Kinnunen, P. K. (1995) Reversibility of the binding of cytochrome c to liposomes. Implications for lipid-protein interactions. *J. Biol. Chem. 270*, 3197−3202.
(92) Rytomaa, M., and Kinnunen, P. K. (1996) Dissociation of cytochrome c from liposomes by histone H1. Comparison with basic peptides. *Biochemistry 35*, 4529−4539.
(93) Kawai, C., Pessoto, F. S., Graves, C. V., Carmona-Ribeiro, A. M., and Nantes, I. L. (2013) Effects of transmembrane potential and pH gradient on the cytochrome c-promoted fusion of mitochondrial mimetic membranes. *J. Bioenerg. Biomembr. 45*, 421−430.
(94) Kagan, V. E., Bayir, H. A., Belikova, N. A., Kapralov, O., Tyurina, Y. Y., Tyurin, V. A., Jiang, J., Stoyanovsky, D. A., Wipf, P., Kochanek, P. M., Greenberger, J. S., Pitt, B., Shvedova, A. A., and Borisenko, G. (2009) Cytochrome c/cardiolipin relations in mitochondria: a kiss of death. *Free Radical Biol. Med. 46*, 1439−1453.
(95) Kapralov, A. A., Kurnikov, I. V., Vlasova, II, Belikova, N. A., Tyurin, V. A., Basova, L. V., Zhao, Q., Tyurina, Y. Y., Jiang, J., Bayir, H., Vladimirov, Y. A., and Kagan, V. E. (2007) The hierarchy of structural transitions induced in cytochrome c by anionic phospholipids determines its peroxidase activation and selective peroxidation during apoptosis in cells. *Biochemistry 46*, 14232−14244.
(96) Jutila, A., Rytomaa, M., and Kinnunen, P. K. (1998) Detachment of cytochrome c by cationic drugs from membranes containing acidic phospholipids: comparison of lidocaine, propranolol, and gentamycin. *Mol. Pharmacol. 54*, 722−732.
(97) Kagan, V. E., Chu, C. T., Tyurina, Y. Y., Cheikhi, A., and Bayir, H. (2014) Cardiolipin asymmetry, oxidation and signaling. *Chem. Phys. Lipids 179*, 64−69.
(98) Radi, R., Sims, S., Cassina, A., and Turrens, J. F. (1993) Roles of catalase and cytochrome c in hydroperoxide-dependent lipid peroxidation and chemiluminescence in rat heart and kidney mitochondria. *Free Radical Biol. Med. 15*, 653−659.
(99) Radi, R., Turrens, J. F., Chang, L. Y., Bush, K. M., Crapo, J. D., and Freeman, B. A. (1991) Detection of catalase in rat heart mitochondria. *J. Biol. Chem. 266*, 22028−22034.

DOI: 10.1021/acs.biochem.5b01385
Biochemistry 2016, 55, 407−428

(100) Radi, R., Turrens, J. F., and Freeman, B. A. (1991) Cytochrome c-catalyzed membrane lipid peroxidation by hydrogen peroxide. *Arch. Biochem. Biophys. 288*, 118−125.
(101) Sinibaldi, F., Fiorucci, L., Patriarca, A., Lauceri, R., Ferri, T., Coletta, M., and Santucci, R. (2008) Insights into cytochrome c-cardiolipin interaction. Role played by ionic strength. *Biochemistry 47*, 6928−6935.
(102) Abe, M., Niibayashi, R., Koubori, S., Moriyama, I., and Miyoshi, H. (2011) Molecular mechanisms for the induction of peroxidase activity of the cytochrome c-cardiolipin complex. *Biochemistry 50*, 8383−8391.
(103) Vladimirov, Y. A., Proskurnina, E. V., Izmailov, D. Y., Novikov, A. A., Brusnichkin, A. V., Osipov, A. N., and Kagan, V. E. (2006) Cardiolipin activates cytochrome c peroxidase activity since it facilitates H(2)O(2) access to heme. *Biochemistry (Moscow) 71*, 998−1005.
(104) Vladimirov, Y. A., Proskurnina, E. V., Izmailov, D. Y., Novikov, A. A., Brusnichkin, A. V., Osipov, A. N., and Kagan, V. E. (2006) Mechanism of activation of cytochrome C peroxidase activity by cardiolipin. *Biochemistry (Moscow) 71*, 989−997.
(105) Huang, Z., Jiang, J., Tyurin, V. A., Zhao, Q., Mnuskin, A., Ren, J., Belikova, N. A., Feng, W., Kurnikov, I. V., and Kagan, V. E. (2008) Cardiolipin deficiency leads to decreased cardiolipin peroxidation and increased resistance of cells to apoptosis. *Free Radical Biol. Med. 44*, 1935−1944.
(106) Belikova, N. A., Vladimirov, Y. A., Osipov, A. N., Kapralov, A. A., Tyurin, V. A., Potapovich, M. V., Basova, L. V., Peterson, J., Kurnikov, I. V., and Kagan, V. E. (2006) Peroxidase activity and structural transitions of cytochrome c bound to cardiolipin-containing membranes. *Biochemistry 45*, 4998−5009.
(107) Patriarca, A., Polticelli, F., Piro, M. C., Sinibaldi, F., Mei, G., Bari, M., Santucci, R., and Fiorucci, L. (2012) Conversion of cytochrome c into a peroxidase: inhibitory mechanisms and implication for neurodegenerative diseases. *Arch. Biochem. Biophys. 522*, 62−69.
(108) Bartesaghi, S., Wenzel, J., Trujillo, M., Lopez, M., Joseph, J., Kalyanaraman, B., and Radi, R. (2010) Lipid peroxyl radicals mediate tyrosine dimerization and nitration in membranes. *Chem. Res. Toxicol. 23*, 821−835.
(109) Folkes, L. K., Bartesaghi, S., Trujillo, M., Radi, R., and Wardman, P. (2012) Kinetics of oxidation of tyrosine by a model alkoxyl radical. *Free Radical Res. 46*, 1150−1156.
(110) Kapetanaki, S. M., Silkstone, G., Husu, I., Liebl, U., Wilson, M. T., and Vos, M. H. (2009) Interaction of carbon monoxide with the apoptosis-inducing cytochrome c-cardiolipin complex. *Biochemistry 48*, 1613−1619.
(111) Spooner, P. J., and Watts, A. (1992) Cytochrome c interactions with cardiolipin in bilayers: a multinuclear magic-angle spinning NMR study. *Biochemistry 31*, 10129−10138.
(112) Hanske, J., Toffey, J. R., Morenz, A. M., Bonilla, A. J., Schiavoni, K. H., and Pletneva, E. V. (2012) Conformational properties of cardiolipin-bound cytochrome c. *Proc. Natl. Acad. Sci. U. S. A. 109*, 125−130.
(113) Balakrishnan, G., Hu, Y., Oyerinde, O. F., Su, J., Groves, J. T., and Spiro, T. G. (2007) A conformational switch to beta-sheet structure in cytochrome c leads to heme exposure. Implications for cardiolipin peroxidation and apoptosis. *J. Am. Chem. Soc. 129*, 504−505.
(114) Pandiscia, L. A., and Schweitzer-Stenner, R. (2015) Coexistence of native-like and non-native partially unfolded ferricytochrome c on the surface of cardiolipin-containing liposomes. *J. Phys. Chem. B 119*, 1334−1349.
(115) O'Brien, E. S., Nucci, N. V., Fuglestad, B., Tommos, C., and Wand, A. J. (2015) Defining the apoptotic trigger: the interaction of cytochrome c and cardiolipin. *J. Biol. Chem. 290*, 30879.
(116) Mandal, A., Hoop, C. L., DeLucia, M., Kodali, R., Kagan, V. E., Ahn, J., and van der Wel, P. C. (2015) Structural Changes and Proapoptotic Peroxidase Activity of Cardiolipin-Bound Mitochondrial Cytochrome c. *Biophys. J. 109*, 1873−1884.
(117) Oellerich, S., Lecomte, S., Paternostre, M., Heimburg, T., and Hildebrandt, P. (2004) Peripheral and Integral Binding of Cytochrome c to Phospholipids Vesicles. *J. Phys. Chem. B 108*, 3871−3878.
(118) Simon, M., Metzinger-Le Meuth, V., Chevance, S., Delalande, O., and Bondon, A. (2013) Versatility of non-native forms of human cytochrome c: pH and micellar concentration dependence. *JBIC, J. Biol. Inorg. Chem. 18*, 27−38.
(119) Sinibaldi, F., Howes, B. D., Piro, M. C., Polticelli, F., Bombelli, C., Ferri, T., Coletta, M., Smulevich, G., and Santucci, R. (2010) Extended cardiolipin anchorage to cytochrome c: a model for protein-mitochondrial membrane binding. *JBIC, J. Biol. Inorg. Chem. 15*, 689−700.
(120) Bergstrom, C. L., Beales, P. A., Lv, Y., Vanderlick, T. K., and Groves, J. T. (2013) Cytochrome c causes pore formation in cardiolipin-containing membranes. *Proc. Natl. Acad. Sci. U. S. A. 110*, 6269−6274.
(121) Firsov, A. M., Kotova, E. A., Korepanova, E. A., Osipov, A. N., and Antonenko, Y. N. (2015) Peroxidative permeabilization of liposomes induced by cytochrome c/cardiolipin complex. *Biochim. Biophys. Acta, Biomembr. 1848*, 767−774.
(122) Gonzalez-Arzola, K., Diaz-Moreno, I., Cano-Gonzalez, A., Diaz-Quintana, A., Velazquez-Campoy, A., Moreno-Beltran, B., Lopez-Rivas, A., and De la Rosa, M. A. (2015) Structural basis for inhibition of the histone chaperone activity of SET/TAF-Ibeta by cytochrome c. *Proc. Natl. Acad. Sci. U. S. A. 112*, 9908−9913.
(123) Batthyany, C., Souza, J. M., Duran, R., Cassina, A., Cervenansky, C., and Radi, R. (2005) Time course and site(s) of cytochrome c tyrosine nitration by peroxynitrite. *Biochemistry 44*, 8038−8046.
(124) Souza, J. M., Castro, L., Cassina, A. M., Batthyany, C., and Radi, R. (2008) Nitrocytochrome c: synthesis, purification, and functional studies. *Methods Enzymol. 441*, 197−215.
(125) Radi, R. (2004) Nitric oxide, oxidants, and protein tyrosine nitration. *Proc. Natl. Acad. Sci. U. S. A. 101*, 4003−4008.
(126) Souza, J. M., Peluffo, G., and Radi, R. (2008) Protein tyrosine nitration–functional alteration or just a biomarker? *Free Radical Biol. Med. 45*, 357−366.
(127) Radi, R. (2013) Protein tyrosine nitration: biochemical mechanisms and structural basis of functional effects. *Acc. Chem. Res. 46*, 550−559.
(128) Alonso, D., Encinas, J. M., Uttenthal, L. O., Bosca, L., Serrano, J., Fernandez, A. P., Castro-Blanco, S., Santacana, M., Bentura, M. L., Richart, A., Fernandez-Vizarra, P., and Rodrigo, J. (2002) Coexistence of translocated cytochrome c and nitrated protein in neurons of the rat cerebral cortex after oxygen and glucose deprivation. *Neuroscience 111*, 47−56.
(129) Cruthirds, D. L., Novak, L., Akhi, K. M., Sanders, P. W., Thompson, J. A., and MacMillan-Crow, L. A. (2003) Mitochondrial targets of oxidative stress during renal ischemia/reperfusion. *Arch. Biochem. Biophys. 412*, 27−33.
(130) Peluffo, G., and Radi, R. (2007) Biochemistry of protein tyrosine nitration in cardiovascular pathology. *Cardiovasc. Res. 75*, 291−302.
(131) Oursler, M. J., Bradley, E. W., Elfering, S. L., and Giulivi, C. (2005) Native, not nitrated, cytochrome c and mitochondria-derived hydrogen peroxide drive osteoclast apoptosis. *Am. J. Physiol. Cell. Physiol. 288*, C156−168.
(132) Nakagawa, H., Komai, N., Takusagawa, M., Miura, Y., Toda, T., Miyata, N., Ozawa, T., and Ikota, N. (2007) Nitration of specific tyrosine residues of cytochrome C is associated with caspase-cascade inactivation. *Biol. Pharm. Bull. 30*, 15−20.
(133) Jang, B., and Han, S. (2006) Biochemical properties of cytochrome c nitrated by peroxynitrite. *Biochimie 88*, 53−58.
(134) Rodriguez-Roldan, V., Garcia-Heredia, J. M., Navarro, J. A., De la Rosa, M. A., and Hervas, M. (2008) Effect of nitration on the physicochemical and kinetic features of wild-type and monotyrosine mutants of human respiratory cytochrome c. *Biochemistry 47*, 12371−12379.

DOI: 10.1021/acs.biochem.5b01385
Biochemistry 2016, 55, 407−428

(135) Ly, H. K., Utesch, T., Diaz-Moreno, I., Garcia-Heredia, J. M., De La Rosa, M. A., and Hildebrandt, P. (2012) Perturbation of the redox site structure of cytochrome c variants upon tyrosine nitration. *J. Phys. Chem. B 116*, 5694−5702.
(136) Tognaccini, L., Ciaccio, C., D'Oria, V., Cervelli, M., Howes, B. D., Coletta, M., Mariottini, P., Smulevich, G., and Fiorucci, L. (2016) Structure-function relationships in human cytochrome c: The role of tyrosine 67. *J. Inorg. Biochem. 155*, 56−66.
(137) Ying, T., Wang, Z. H., Lin, Y. W., Xie, J., Tan, X., and Huang, Z. X. (2009) Tyrosine-67 in cytochrome c is a possible apoptotic trigger controlled by hydrogen bonds via a conformational transition. *Chem. Commun. (Cambridge, U. K.)*, 4512−4514.
(138) Garcia-Heredia, J. M., Diaz-Moreno, I., Nieto, P. M., Orzáez, M., Kocanis, S., Teixeira, M., Perez-Paya, E., Diaz-Quintana, A., and De la Rosa, M. A. (2010) Nitration of tyrosine 74 prevents human cytochrome c to play a key role in apoptosis signaling by blocking caspase-9 activation. *Biochim. Biophys. Acta, Bioenerg. 1797*, 981−993.
(139) Alvarez-Paggi, D., Castro, M. A., Tortora, V., Castro, L., Radi, R., and Murgida, D. H. (2013) Electrostatically driven second-sphere ligand switch between high and low reorganization energy forms of native cytochrome c. *J. Am. Chem. Soc. 135*, 4389−4397.
(140) Diaz-Moreno, I., Garcia-Heredia, J. M., Diaz-Quintana, A., Teixeira, M., and De la Rosa, M. A. (2011) Nitration of tyrosines 46 and 48 induces the specific degradation of cytochrome c upon change of the heme iron state to high-spin. *Biochim. Biophys. Acta, Bioenerg. 1807*, 1616−1623.
(141) Garcia-Heredia, J. M., Diaz-Quintana, A., Salzano, M., Orzáez, M., Perez-Paya, E., Teixeira, M., De la Rosa, M. A., and Diaz-Moreno, I. (2011) Tyrosine phosphorylation turns alkaline transition into a biologically relevant process and makes human cytochrome c behave as an anti-apoptotic switch. *JBIC, J. Biol. Inorg. Chem. 16*, 1155−1168.
(142) Rajagopal, B. S., Edzuma, A. N., Hough, M. A., Blundell, K. L., Kagan, V. E., Kapralov, A. A., Fraser, L. A., Butt, J. N., Silkstone, G. G., Wilson, M. T., Svistunenko, D. A., and Worrall, J. A. (2013) The hydrogen-peroxide-induced radical behaviour in human cytochrome c-phospholipid complexes: implications for the enhanced pro-apoptotic activity of the G41S mutant. *Biochem. J. 456*, 441−452.
(143) Morison, I. M., Cramer Borde, E. M., Cheesman, E. J., Cheong, P. L., Holyoake, A. J., Fichelson, S., Weeks, R. J., Lo, A., Davies, S. M., Wilbanks, S. M., Fagerlund, R. D., Ludgate, M. W., da Silva Tatley, F. M., Coker, M. S., Bockett, N. A., Hughes, G., Pippig, D. A., Smith, M. P., Capron, C., and Ledgerwood, E. C. (2008) A mutation of human cytochrome c enhances the intrinsic apoptotic pathway but causes only thrombocytopenia. *Nat. Genet. 40*, 387−389.
(144) Capdevila, D. A., Marmisolle, W. A., Tomasina, F., Demicheli, V., Portela, M., Radi, R., and Murgida, D. H. (2015) Specific methionine oxidation of cytochrome c in complexes with zwitterionic lipids by hydrogen peroxide: potential implications for apoptosis. *Chem. Sci. 6*, 705−713.
(145) Azzi, A., Montecucco, C., and Richter, C. (1975) The use of acetylated ferricytochrome c for the detection of superoxide radicals produced in biological membranes. *Biochem. Biophys. Res. Commun. 65*, 597−603.
(146) Kim, S. C., Sprung, R., Chen, Y., Xu, Y., Ball, H., Pei, J., Cheng, T., Kho, Y., Xiao, H., Xiao, L., Grishin, N. V., White, M., Yang, X. J., and Zhao, Y. (2006) Substrate and functional diversity of lysine acetylation revealed by a proteomics survey. *Mol. Cell 23*, 607−618.
(147) Osman, C., Voelker, D. R., and Langer, T. (2011) Making heads or tails of phospholipids in mitochondria. *J. Cell Biol. 192*, 7−16.
(148) Salamon, Z., and Tollin, G. (1997) Interaction of horse heart cytochrome c with lipid bilayer membranes: effects on redox potentials. *J. Bioenerg. Biomembr. 29*, 211−221.
(149) Trusova, V. M., Gorbenko, G. P., Molotkovsky, J. G., and Kinnunen, P. K. (2010) Cytochrome c-lipid interactions: new insights from resonance energy transfer. *Biophys. J. 99*, 1754−1763.
(150) Capdevila, D. A., Marmisolle, W. A., Williams, F. J., and Murgida, D. H. (2013) Phosphate mediated adsorption and electron transfer of cytochrome c. A time-resolved SERR spectroelectrochemical study. *Phys. Chem. Chem. Phys. 15*, 5386−5394.
(151) Marmisolle, W. A., Capdevila, D. A., de la Llave, E., Williams, F. J., and Murgida, D. H. (2013) Self-assembled monolayers of NH2-terminated thiolates: order, pKa, and specific adsorption. *Langmuir 29*, 5351−5359.
(152) Wang, B., Zhang, J. J., Pan, Z. Y., Tao, X. Q., and Wang, H. S. (2009) A novel hydrogen peroxide sensor based on the direct electron transfer of horseradish peroxidase immobilized on silica-hydroxyapatite hybrid film. *Biosens. Bioelectron. 24*, 1141−1145.
(153) Sun, H., Hu, N., and Ma, H. (2000) Direct Electrochemistry of Hemoglobin in Polyacrylamide Hydrogel Films on Pyrolytic Graphite Electrodes. *Electroanalysis 12*, 1064−1070.
(154) Giorgio, M., Trinei, M., Migliaccio, E., and Pelicci, P. G. (2007) Hydrogen peroxide: a metabolic by-product or a common mediator of ageing signals? *Nat. Rev. Mol. Cell Biol. 8*, 722−728.
(155) Radi, R., Thomson, L., Rubbo, H., and Prodanov, E. (1991) Cytochrome c-catalyzed oxidation of organic molecules by hydrogen peroxide. *Arch. Biochem. Biophys. 288*, 112−117.
(156) De Biase, P. M., Paggi, D. A., Doctorovich, F., Hildebrandt, P., Estrin, D. A., Murgida, D. H., and Marti, M. A. (2009) Molecular basis for the electric field modulation of cytochrome C structure and function. *J. Am. Chem. Soc. 131*, 16248−16256.
(157) Capdevila, D. A., Alvarez-Paggi, D., Castro, M. A., Tortora, V., Demicheli, V., Estrin, D. A., Radi, R., and Murgida, D. H. (2014) Coupling of tyrosine deprotonation and axial ligand exchange in nitrocytochrome c. *Chem. Commun. (Cambridge, U. K.) 50*, 2592−2594.
(158) Diederix, R. E., Ubbink, M., and Canters, G. W. (2002) Peroxidase activity as a tool for studying the folding of c-type cytochromes. *Biochemistry 41*, 13067−13077.
(159) Clarke, R. J. (2001) The dipole potential of phospholipid membranes and methods for its detection. *Adv. Colloid Interface Sci. 89*−*90*, 263−281.
(160) Marcus, R. A. (1964) Chemical and Electrochemical Electron-Transfer Theory. *Annu. Rev. Phys. Chem. 15*, 155−196.
(161) Marcus, R. A. (1993) Electron Transfer Reactions in Chemistry: Theory and Experiment (Nobel Lecture). *Angew. Chem., Int. Ed. Engl. 32*, 1111−1121.
(162) Murgida, D. H., and Hildebrandt, P. (2008) Disentangling interfacial redox processes of proteins by SERR spectroscopy. *Chem. Soc. Rev. 37*, 937−945.
(163) Murgida, D. H., and Hildebrandt, P. (2004) Electron-transfer processes of cytochrome C at interfaces. New insights by surface-enhanced resonance Raman spectroscopy. *Acc. Chem. Res. 37*, 854−861.
(164) Kranich, A., Ly, H. K., Hildebrandt, P., and Murgida, D. H. (2008) Direct observation of the gating step in protein electron transfer: electric-field-controlled protein dynamics. *J. Am. Chem. Soc. 130*, 9844−9848.
(165) Murgida, D. H., and Hildebrandt, P. (2001) Heterogeneous Electron Transfer of Cytochrome c on Coated Silver Electrodes. Electric Field Effects on Structure and Redox Potential. *J. Phys. Chem. B 105*, 1578−1586.
(166) Koppenol, W. H., Rush, J. D., Mills, J. D., and Margoliash, E. (1991) The dipole moment of cytochrome c. *Mol. Biol. Evol. 8*, 545−558.
(167) Alvarez-Paggi, D., Martin, D. F., DeBiase, P. M., Hildebrandt, P., Marti, M. A., and Murgida, D. H. (2010) Molecular basis of coupled protein and electron transfer dynamics of cytochrome c in biomimetic complexes. *J. Am. Chem. Soc. 132*, 5769−5778.
(168) Paggi, D. A., Martín, D. F., Kranich, A., Hildebrandt, P., Martí, M. A., and Murgida, D. H. (2009) Computer simulation and SERR detection of cytochrome c dynamics at SAM-coated electrodes. *Electrochim. Acta 54*, 4963−4970.
(169) Ly, H. K., Marti, M. A., Martin, D. F., Alvarez-Paggi, D., Meister, W., Kranich, A., Weidinger, I. M., Hildebrandt, P., and Murgida, D. H. (2010) Thermal fluctuations determine the electron-transfer rates of cytochrome c in electrostatic and covalent complexes. *ChemPhysChem 11*, 1225−1235.

DOI: 10.1021/acs.biochem.5b01385
Biochemistry 2016, 55, 407−428

(170) Alvarez-Paggi, D., Meister, W., Kuhlmann, U., Weidinger, I., Tenger, K., Zimanyi, L., Rakhely, G., Hildebrandt, P., and Murgida, D. H. (2013) Disentangling electron tunneling and protein dynamics of cytochrome c through a rationally designed surface mutation. *J. Phys. Chem. B 117*, 6061−6068.
(171) Battistuzzi, G., Bortolotti, C. A., Bellei, M., Di Rocco, G., Salewski, J., Hildebrandt, P., and Sola, M. (2012) Role of Met80 and Tyr67 in the low-pH conformational equilibria of cytochrome c. *Biochemistry 51*, 5967−5978.
(172) Berghuis, A. M., Guillemette, J. G., McLendon, G., Sherman, F., Smith, M., and Brayer, G. D. (1994) The role of a conserved internal water molecule and its associated hydrogen bond network in cytochrome c. *J. Mol. Biol. 236*, 786−799.
(173) Feinberg, B. A., Petro, L., Hock, G., Qin, W., and Margoliash, E. (1999) Using entropies of reaction to predict changes in protein stability: tyrosine-67-phenylalanine variants of rat cytochrome c and yeast Iso-1 cytochromes c. *J. Pharm. Biomed. Anal. 19*, 115−125.
(174) Zhou, P., Tian, F., Lv, F., and Shang, Z. (2009) Geometric characteristics of hydrogen bonds involving sulfur atoms in proteins. *Proteins: Struct., Funct., Genet. 76*, 151−163.
(175) Lange, C., and Hunte, C. (2002) Crystal structure of the yeast cytochrome bc1 complex with its bound substrate cytochrome c. *Proc. Natl. Acad. Sci. U. S. A. 99*, 2800−2805.
(176) Pelletier, H., and Kraut, J. (1992) Crystal structure of a complex between electron transfer partners, cytochrome c peroxidase and cytochrome c. *Science 258*, 1748−1755.
(177) Roberts, V. A., and Pique, M. E. (1999) Definition of the interaction domain for cytochrome c on cytochrome c oxidase. III. Prediction of the docked complex by a complete, systematic search. *J. Biol. Chem. 274*, 38051−38060.
(178) Khoa Ly, H. K., Sezer, M., Wisitruangsakul, N., Feng, J. J., Kranich, A., Millo, D., Weidinger, I. M., Zebger, I., Murgida, D. H., and Hildebrandt, P. (2011) Surface-enhanced vibrational spectroscopy for probing transient interactions of proteins with biomimetic interfaces: electric field effects on structure, dynamics and function of cytochrome c. *FEBS J. 278*, 1382−1390.
(179) Weidinger, I. M., Murgida, D. H., Dong, W. F., Mohwald, H., and Hildebrandt, P. (2006) Redox processes of cytochrome c immobilized on solid supported polyelectrolyte multilayers. *J. Phys. Chem. B 110*, 522−529.
(180) Oellerich, S., Wackerbarth, H., and Hildebrandt, P. (2002) Spectroscopic Characterization of Nonnative Conformational States of Cytochrome c. *J. Phys. Chem. B 106*, 6566−6580.
(181) Dopner, S., Hildebrandt, P., Rosell, F. I., Mauk, A. G., von Walter, M., Buse, G., and Soulimane, T. (1999) The structural and functional role of lysine residues in the binding domain of cytochrome c in the electron transfer to cytochrome c oxidase. *Eur. J. Biochem. 261*, 379−391.
(182) De Biase, P. M., Doctorovich, F., Murgida, D. H., and Estrin, D. A. (2007) Electric field effects on the reactivity of heme model systems. *Chem. Phys. Lett. 434*, 121−126.
(183) Sela, M., Schechter, B., Schechter, I., and Borek, F. (1967) Antibodies to sequential and conformational determinants. *Cold Spring Harbor Symp. Quant. Biol. 32*, 537−545.
(184) Jemmerson, R. (1987) Antigenicity and native structure of globular proteins: low frequency of peptide reactive antibodies. *Proc. Natl. Acad. Sci. U. S. A. 84*, 9180−9184.
(185) Spangler, B. D. (1991) Binding to native proteins by antipeptide monoclonal antibodies. *J. Immunol. 146*, 1591−1595.
(186) Liu, X., Kim, C. N., Yang, J., Jemmerson, R., and Wang, X. (1996) Induction of apoptotic program in cell-free extracts: requirement for dATP and cytochrome c. *Cell 86*, 147−157.
(187) Jemmerson, R., and Paterson, Y. (1986) Mapping epitopes on a protein antigen by the proteolysis of antigen-antibody complexes. *Science 232*, 1001−1004.
(188) Bakan, A., Kapralov, A. A., Bayir, H., Hu, F., Kagan, V. E., and Bahar, I. (2015) Inhibition of Peroxidase Activity of Cytochrome c: De Novo Compound Discovery and Validation. *Mol. Pharmacol. 88*, 421.
(189) Koonin, E. V., and Aravind, L. (2002) Origin and evolution of eukaryotic apoptosis: the bacterial connection. *Cell Death Differ. 9*, 394−404.
(190) Kluck, R. M., Ellerby, L. M., Ellerby, H. M., Naiem, S., Yaffe, M. P., Margoliash, E., Bredesen, D., Mauk, A. G., Sherman, F., and Newmeyer, D. D. (2000) Determinants of cytochrome c pro-apoptotic activity. The role of lysine 72 trimethylation. *J. Biol. Chem. 275*, 16127−16133.
(191) Ascenzi, P., Marino, M., Ciaccio, C., Santucci, R., and Coletta, M. (2014) Reductive nitrosylation of the cardiolipin-ferric cytochrome c complex. *IUBMB Life 66*, 438−447.
(192) Ott, M., Robertson, J. D., Gogvadze, V., Zhivotovsky, B., and Orrenius, S. (2002) Cytochrome c release from mitochondria proceeds by a two-step process. *Proc. Natl. Acad. Sci. U. S. A. 99*, 1259−1263.
(193) Tam, Z. Y., Cai, Y. H., and Gunawan, R. (2010) Elucidating cytochrome C release from mitochondria: insights from an in silico three-dimensional model. *Biophys. J. 99*, 3155−3163.
(194) Garcia-Heredia, J. M., Diaz-Moreno, I., Diaz-Quintana, A., Orzáez, M., Navarro, J. A., Hervas, M., and De la Rosa, M. A. (2012) Specific nitration of tyrosines 46 and 48 makes cytochrome c assemble a non-functional apoptosome. *FEBS Lett. 586*, 154−158.
(195) Battistuzzi, G., Borsari, M., and Sola, M. (2001) Redox properties of cytochrome c. *Antioxid. Redox Signaling 3*, 279−291.

DOI: 10.1021/acs.biochem.5b01385
Biochemistry 2016, 55, 407−428